

---

# Properties of Magneticum Disk Galaxies in the Context of Modified Newtonian Dynamics

---

## Eigenschaften von Scheibengalaxien in Magneticum im Kontext von Modifizierter Newtonscher Dynamik

Alexander Mayer

---



München 2019



# Properties of Magneticum Disk Galaxies in the Context of Modified Newtonian Dynamics

---

## Eigenschaften von Scheibengalaxien in Magneticum im Kontext von Modifizierter Newtonscher Dynamik

Bachelor-Arbeit  
an der  
Ludwig-Maximilians-Universität München

eingereicht von

**Alexander Mayer**

(Matr. Nr.: 11557369)

geboren am 26.03.1998 in München

betreut von  
PD Dr. Klaus Dolag

und  
Dr. Adelheid Teklu

München, September 6, 2019

Evaluator: PD Dr. Klaus Dolag

Tag der mündlichen Prüfung: 13.08.2019

# Contents

1	Introduction . . . . .	i
2	Theoretical foundations . . . . .	iii
2.1	A brief history of the standard model . . . . .	iii
2.2	Rotation curves . . . . .	viii
2.3	Dark matter halos . . . . .	x
2.4	Modified Newtonian Dynamics . . . . .	xii
2.5	Acceleration relations . . . . .	xvi
2.6	The laws of galactic rotation . . . . .	xviii
2.7	The Magneticum simulation . . . . .	xix
3	MOND in Magneticum . . . . .	xx
3.1	Rotation curves of Magneticum galaxies . . . . .	xx
3.2	TFR in Magneticum . . . . .	xxvi
3.3	MDAR and RAR in Magneticum . . . . .	xxviii
3.4	2D maps of rotational velocity . . . . .	xxxii
3.5	2D predictions of velocity from the gravitational potential . . . . .	xxxiii
3.6	MDAR for individual galaxies . . . . .	xxxix
4	Mass models, dark matter halos and the MDAR . . . . .	xl
4.1	Mass profiles of Magneticum galaxies . . . . .	xl
4.2	Baryonic mass profiles from MOND and halo shapes . . . . .	xli
4.3	Acceleration laws in a Milky Way model . . . . .	xliii
4.4	General results for mass distributions and the MDAR . . . . .	xlvi
5	Summary . . . . .	xlviii
5.1	Laws of galactic rotation in Magneticum . . . . .	xlviii
5.2	Mass distributions of galaxies in the context of the MDAR . . . . .	xlix
6	Conclusions and outlook . . . . .	l
6.1	Implications . . . . .	l
6.2	Other tests for MOND . . . . .	li
6.3	Building upon this thesis . . . . .	li
7	Appendix . . . . .	lii
7.1	Simulating observation . . . . .	lii
7.2	Additional plots . . . . .	liv

# 1 Introduction

In the standard model of cosmology ( $\Lambda$ CDM), ordinary matter - mainly protons, neutrons and electrons - that everything we see each day is made out of, only forms a quite small part of the whole mass of the universe, less than 5 %. The rest is fittingly called 'dark', where the name not only reflects that the other 95 % do not emit any form of light, but also that we know almost nothing about what they are fundamentally made of.

69 % bare the name **dark energy**, but this is really only a name given to a property that accelerates the expansion of the universe. While it is suspected to be a form of negative pressure/energy of the vacuum, no calculations from quantum physics have yielded reasonable agreement with astronomical observations - the prediction made by quantum field theory is far too large.

The remaining 26 % are what is called **dark matter**. It is thought to be largely responsible for the formation of structure in the universe and the internal dynamics of galaxy clusters as well as individual galaxies. One particular oddity of the universe is the high speed at which gas (mostly hydrogen) and stars move around the center of their host galaxies. The laws of gravity predict a drop-off of the velocity in the outer regions: Objects that are further away from the center should move slower. But this is not the case. Instead, the speed stays about constant when one looks further and further away from the center. This discrepancy can be explained by the stars of the galaxy sitting in a so-called 'halo' of dark matter, which is much more massive than the visible part and exerts a strong pull on the outer stars. To balance this, these outer stars need higher speeds to have a circular orbit.

In the absence of a direct detection of dark matter, alternatives have been put forth that do not rely on dark matter particles that might possibly not exist. One of the most persistent is **MODified Newtonian Dynamics** or **MOND**. As the name implies, MOND proposes a modification of Newton's second law or his law of gravitation. While the effects of this change are supposed to be negligible in everyday life on earth and the solar system, they should significantly alter the dynamics in regions of low acceleration. A characteristic scale under which MOND deviates strongly from Newtonian dynamics is usually taken to be  $\sim 1.2 * 10^{-10} \frac{m}{s^2}$ .

The outer regions of most galaxies and even the inner regions of mass-poor ones can easily reach accelerations below this value. Therefore, under MOND, the gravitational pull inward is also stronger there than expected from visible matter and Newtonian physics, which provides an alternative explanation for the aforementioned flat rotation curves.

How can one distinguish between  $\Lambda$ CDM and MOND? First of all, the universe is way bigger than individual galaxies. A satisfying cosmology - a model of the whole universe and its evolution - has yet to be constructed from MOND, while the  $\Lambda$ CDM cosmology has been making correct predictions for decades now. MOND also appears to have prob-

lems on the scale of clusters of galaxies [McGaugh (2015)], the largest gravitationally bound structures in the universe, and it seems as though MOND might need to rely on a certain but smaller amount of dark matter, too.

Wide binary stars have also been proposed to be a suitable laboratory to test modified gravity, since the mutual acceleration between the two stars can reach very low values.

But the differences between the two models can also be investigated on the scale of galaxies. Proponents of MOND argue that the dynamics of the gas in galaxies follow the distribution of luminous matter much more closely than is to be expected with dark matter involved. MOND also predicts a particular relation between the total acceleration calculated from observations of the orbits of stars and gas and the acceleration that visible matter provides. This relation seems to actually be present in measurements of galaxies, but could of course also be explained by a particular interplay of dark and ordinary matter.

The question then arises whether these predictions are actually exclusively made by MOND. The correct tool to answer this question are cosmological simulations, which have become invaluable in astronomy for their ability to model the whole evolution of the universe. They allow researchers to test whether the assumptions of current theories are correct: You start with conditions thought to have been present in the early universe and then let this simulated universe evolve under assumed principles. If you then end up with something that looks similar to the real universe, then the models appear to be at least consistent with reality.

If instead the features of simulated galaxies differ substantially from real ones - for example because they do not show a certain acceleration-scaling - then either the model was wrong, or the simulation does not represent the model accurately.

Whether the acceleration-relation predicted by MOND also appears in  $\Lambda$ CDM-simulations has been investigated before [Navarro et al. (2017), Dutton et al. (2019)], but not yet in the *Magneticum* simulation of the CAST-group at USM.

In this bachelor thesis, I will take a look at the dynamics of spiral galaxies in the *Magneticum* simulation and attempt to find out if predictions of MOND also hold true for its galaxies.

But neither outcome can really be conclusive:

- a) If the phenomenology of MOND is also present in this simulation based on  $\Lambda$ CDM, then they predict the same thing - making them indistinguishable in this regard.
- b) If it is **not** present, then this might not signify the failure of the model, but instead only of the simulation, telling us nothing about reality.

Nonetheless, both outcomes can provide valuable information:

- a) The appearance of MOND laws in another  $\Lambda$ CDM simulation would be highly consistent with the idea that MOND is purely empirical, with its observational basis being galaxies which actually come to be and work in a framework of dark matter.
- b) A failure to detect such features could help to find flaws in the current simulation, which can lead to improvement in the future.

The existence of dark matter is fundamental to the viability of the standard model. Without it, there are no galaxies, clusters behave very differently and more. Therefore showing the incompatibility of galactic dynamics with the idea of dark matter would have substantial implications. While the lack of detection of dark matter candidates can never be proof against its existence - maybe we were just looking for the wrong particle in the wrong place? -, the existence of objects and relations which  $\Lambda$ CDM cannot account for would strongly disfavor dark matter as the answer.

## 2 Theoretical foundations

In this section, I will summarize the theoretical foundations and associated observations that are fundamental for the rest of the thesis. First I am going to give an overview of the history and ideas behind  $\Lambda$ CDM. After a brief introduction to the theory and measurement of rotation curves I will then discuss how their appearance can be explained by dark matter halos. Afterwards, MOND is introduced as an alternative solution, looking at its history and foundations. I will move on to acceleration-relations predicted by MOND. Lastly, I will take a brief look at the basics of the Magneticum simulation.

### 2.1 A brief history of the standard model

In the year 1905, Albert Einstein published 'On the electrodynamics of moving bodies' [Einstein (1905)], the paper that introduced the world to his special theory of relativity. With two postulates - that the speed of light  $c$  is the same in all inertial reference frames and that all laws of physics are the same in all mutually uniformly moving reference frames - he solved the problems raised by the null-result of the Michelson-Morley experiment<sup>1</sup> and abolished the idea of an ether. This theory also gave more accurate predictions of the Doppler-shift for light and stellar aberration and predicted the now well-measured time dilation and length contraction.

Special relativity suffered from a central problem, however: It is irreconcilable with gravitation<sup>2</sup>. This lead Einstein to develop the general theory of relativity, which explains gravity as a manifestation of the mutual interaction of mass-energy and the geometry of space time.

One consequence of Einstein's field equations

$$G_{\mu\nu} \equiv R_{\mu\nu} - \frac{1}{2}Rg_{\mu\nu} = \frac{8\pi G}{c^4}T_{\mu\nu} \quad (1)$$

---

<sup>1</sup>The Michelson-Morley experiment was intended to detect motion of earth relative to the luminiferous ether, which was thought to be a medium for light waves. The paper is available under [https://en.wikisource.org/wiki/The\\_Relative\\_Motion\\_of\\_the\\_Earth\\_and\\_the\\_Luminiferous\\_Ether](https://en.wikisource.org/wiki/The_Relative_Motion_of_the_Earth_and_the_Luminiferous_Ether).

<sup>2</sup>Misner, C.W. , Thorne, K.S. , Wheeler, J.A. (2017). *Gravitation*. Princeton University Press, 2017 edition. p.177

is that the universe should continually be expanding or contracting<sup>3</sup> - an idea that, at the time of formulation, was not deemed to be correct. To preserve the original idea of the theory only one modification was possible: Adding a factor to the left side of (1):

$$G_{\mu\nu} \rightarrow G_{\mu\nu} + \Lambda g_{\mu\nu} \quad (2)$$

which we know today as the **cosmological constant**. With this factor introduced, the equations could give rise to a static universe, but now included some form of 'vacuum energy' that resulted in curvature when no other matter-energy was actually present. But the idea of an expanding universe turned out to be correct when Edwin Hubble observed the redshifts of distant Cepheids [Hubble (1929)] and showed that their host galaxies are moving away from us at a speed which is proportional to their distance:

$$v = H_0 * r \quad (3)$$

The constant of proportionality  $H_0$  is called **Hubble's constant** (although it is really only a constant for one moment in cosmic time). The formula above is known as **Hubble's law** and can be used to ascertain distances on the largest scales in the universe. It also lead to the convention of referring to ages in the universe by their values of redshift  $z$ , since light takes a certain amount of time to reach us from any other point in the universe and the emitter is also redshifted proportional to its distance.

Subsequently, Einstein realized that the introduction of the cosmological constant was a mistake - later calling this act his 'greatest blunder' - because he could have predicted the expansion of the universe before it was observed.

Instead, Alexander Friedmann [Friedmann (1922)] and Georges Lemaître [Lemaître (1927)] independently arrived at the conclusion of a non-static universe from Einstein's equations by inserting the stress energy tensor of a homogeneous and isotropic universe ('cosmological principle'). A-priori different scenarios of the history and future are possible through the **Friedmann equations** for the universe:

$$H^2 = \left(\frac{\dot{a}}{a}\right)^2 = \frac{8\pi G}{3}\rho - \frac{Kc^2}{a^2} + \frac{\Lambda}{3} \quad (4)$$

$$\dot{H} + H^2 = \frac{\ddot{a}}{a} = -\frac{4\pi G}{3}\left(\rho + \frac{3P}{c^2}\right) + \frac{\Lambda}{3} \quad (5)$$

Here,  $H$  is the Hubble 'constant',  $a$  is the dimensionless **scale parameter** that describes the relative size of the universe,  $K$  is a curvature parameter,  $\rho$  is the mean density of mass-energy and  $P$  is pressure; all as functions of time only. The scale parameter can be related to redshift through  $a = \frac{1}{1+z}$ . There is a certain value for the mean density, known as the **critical density**, that describes a **flat** universe ( $K=0$ ), for  $\Lambda = 0$  given by:

$$\rho_{cr} = \frac{3H_0^2}{8\pi G} \quad (6)$$

---

<sup>3</sup>Gravitation p.409

Defining a relative density  $\Omega \equiv \frac{\rho}{\rho_{cr}}$  allows us to write  $K = (\frac{H_0}{c})^2(\Omega - 1)$ , relating curvature to mass-energy density.

The scenarios for different values of the density are illustrated here:

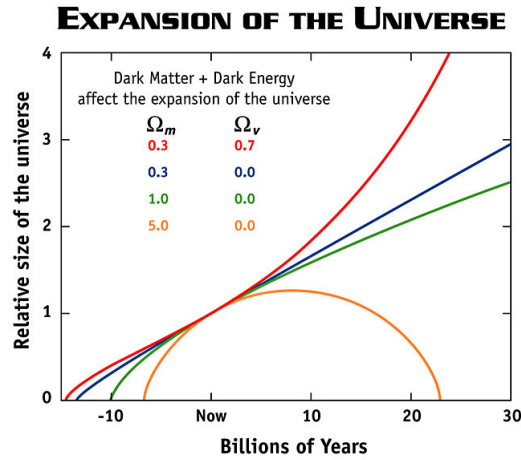


**Fig. 1:** Different scenarios for the universe depending on density parameters. The red curve appears to be the universe we live in. Taken from [https://map.gsfc.nasa.gov/universe/bb\\_concepts\\_exp.html](https://map.gsfc.nasa.gov/universe/bb_concepts_exp.html).

In combination with the observation that the universe is indeed expanding, the work of Friedmann and Lemaître lead to the '**Big Bang**' theory (BBT) (originally a derogatory name invented by Fred Hoyle, a proponent of 'Steady State' theory): From the continual expansion of the universe it follows that it started out in a very hot and dense state.

George Gamow, Ralph Alpher and Robert Herman [Gamow (1948), Alpher and Herman (1948)] predicted in 1948 that this state should have left a mark on the universe: At the earliest times, the universe would have been so hot, so full of photons, that they prevented atoms from forming through their interaction with electrons (Thomson scattering). But at some point, when the universe was about 380000 years old, it would have cooled down sufficiently for neutral atoms to form. The photons would then have been released and still be visible today, redshifted into the microwave range, as a kind of afterglow of this event known as **Recombination**.

This **Cosmic Microwave Background (CMB)**, a ubiquitous, nearly isotropic black body radiation with a temperature of  $(2.72548 \pm 0.00057)K$  [Fixsen (2009)] was found 16 years later by the radio astronomers Arno Penzias and Robert Wilson, working at Bell Labs [Penzias and Wilson (1965)]. This was a clear confirmation of a prediction made by the BBT, but no static theory of the universe. The BBT made other successful predictions, too, such as the proportion of Helium in the universe<sup>4</sup>.

There were still problems left, however. Clearly, there is large-scale structure in the universe: Galaxy clusters on one hand and huge voids with almost no matter on the

<sup>4</sup>Schneider, P. (2008). *Einführung in die Extragalaktische Astronomie und Kosmologie*. Springer. p.165

other. But the anisotropies in the CMB, from which the anisotropies today must have followed are only on the order of  $\sim 0.0005K$ , so the relative differences are  $\sim 10^{-5}$ . These could not have grown into the structures we see today<sup>5</sup>.

Earlier observations of the Coma galaxy cluster by Fritz Zwicky [Zwicky (1933)] suggested that they are lacking mass - luminosity observations in combination with estimates of Mass-to-light ratios (**MLRs**) of stars were not able to explain how the outer galaxies of such clusters could move at the high speeds they have. Velocity measurements made on smaller scales - in individual galaxies - made among others by Jacobus Kapteyn [Kapteyn (1922)], also hinted at the fact that according to the laws of gravity, these galaxies did not nearly have enough mass to produce such high speeds for stars in the outer regions. He already used the name **dark matter (DM)** for this missing mass.

Of course this missing mass could in theory be non-luminous objects, such as planets, brown dwarfs and stellar black holes (this would be the idea of **MASSIVE Compact Halo Objects** or **MACHOs**). But the discrepancies turned out to be very large - for example, according to modern models, the central region of the Coma Cluster would need MLRs of  $\sim 350M_{\odot}/L_{\odot}$  [Merritt (1987)]. Big Bang nucleosynthesis also does not allow for this much baryonic matter<sup>6</sup> (somewhat confusingly, electrons are included with their parent atoms as baryonic matter in this context, even though they are of course leptons).

Therefore the consensus today is that dark matter is actually something very different to 'ordinary' matter - it seems to only interact gravitationally with baryonic matter or perhaps through the weak interaction, but not at all with electromagnetic radiation (hence the attribute 'dark' is appropriate). Ideas for the nature of dark matter vary: Candidates include Weakly Interacting Massive Particles or WIMPs, axions and more. There is also the question of whether dark matter is primarily 'cold', 'warm' or 'hot' - that is, how large its free streaming length is in comparison to a protogalaxy. The standard model of cosmology includes it as **Cold Dark Matter (CDM)**, so the speed of these particles is thought to be way lower than the speed of light in this model. With **cold DM**, structures form bottom up, from small to large structures, in accordance with observations<sup>7</sup>.

This CDM can now explain how the small anisotropies in the CMB could grow into the large ones of the universe today<sup>8</sup>: Before Recombination, dark matter particles had already settled in overdense regions in the CMB ('**seeding**') and attracted baryons gravitationally. The dark matter is not visible in the CMB - it does not interact with light! - but the relative anisotropies in the dark matter density were much larger than the ones in the CMB.

This allowed large-scale structure to form and is also responsible for the existence of galaxies: The dark matter coalesced into halos and baryonic matter then falls into these, forming galaxies. While ordinary matter can radiate away heat, this is not possible for CDM. Loss of energy in combination with preservation of angular momentum leads to

---

<sup>5</sup>Einführung in die Extragalaktische Physik und Kosmologie p.282

<sup>6</sup>Unsöld, A. , Baschek, B. (2002). *Der neue Kosmos*. Springer Spektrum, seventh edition. p.497 et sqq.

<sup>7</sup>Einführung in die Extragalaktische Physik und Kosmologie p.286

<sup>8</sup>Einführung in die Extragalaktische Physik und Kosmologie p.282

the existence of disk galaxies, while their halos are still approximately spherical. However, the halos are not totally unaffected by galaxy formation and some dark matter is dragged inwards with the baryons; this is known as **adiabatic contraction** and leads to halos being flattened from sphericity<sup>9</sup>.

Since in general relativity, more mass-energy equals more curvature and the amount of curvature is tantamount to the evolution of the universe, the presence of dark matter has a huge effect on cosmology. However, measurements of the CMB reveal that the universe has a flat shape and even with added dark matter, the universe lacks density for such a scenario [Planck Collaboration et al. (2018)]. This fact, in combination with the observed acceleration of the expansion of the universe [Riess et al. (1998)], which is not possible for  $\Lambda=0$ , lead to a revival of the cosmological constant in the form of 'dark energy'. The idea of 'vacuum energy' now seemed to have legitimacy from quantum field theory, where the ground state of the vacuum indeed does not have zero energy. That calculations based on quantum field theory produce a value that is many orders of magnitude greater than the observed value for  $\Lambda$  is still an unsolved problem, however [Weinberg (1989)].

The incorporation of the cosmological constant and cold dark matter lead to the standard model of cosmology being referred to as  $\Lambda$ CDM. Modern values for the relative densities of the different components are [Planck Collaboration et al. (2018)]:

$$\Omega_\Lambda = 0.6889 \pm 0.0056 \text{ Dark energy}$$

$$\Omega_m = 0.3111 \pm 0.0056 \text{ All matter}$$

$$\Omega_b h^2 = 0.02242 \pm 0.00014 \text{ Baryonic matter}$$

The factor h is defined by  $H_0 = h * 100 km / (s * Mpc)$ . This factor is introduced because the Hubble constant is not known very precisely. This same source finds

$$H_0 = 67.66 \pm 0.42.$$

$\Lambda$ CDM still suffers from some problems, such as the horizon- and flatness problem, but cosmic inflation seems to be a good solution to both of these<sup>10</sup>. Other than that, the standard model has made many correct predictions for the properties of the CMB and the evolution of the universe as a whole.

This thesis will concentrate on the predictions of  $\Lambda$ CDM on the scale of galaxies: Cosmological simulations, another principal topic of the thesis, show the formation of particular dark matter profiles. The form of these halos is hugely important to the dynamics of the galaxy: Without dark matter,  $\Lambda$ CDM can not explain how high velocities in regions far from galactic centers come to be.

We will now take a more in-depth look at rotation curves and their theoretical foundation.

---

<sup>9</sup>Mo, H. , van den Bosch, F. , White, S. (2010). *Galaxy Formation and Evolution*. Cambridge University Press. p.501 et sqq.

<sup>10</sup>Einführung in die Extragalaktische Physik und Kosmologie. p.172 et sqq.

## 2.2 Rotation curves

Newton's law of gravitation

$$\mathbf{F} = -\frac{GmM}{r^3}\mathbf{r} \quad (7)$$

(here for a point-mass at the origin) has as a consequence that the force field outside a spherically symmetric distribution of matter is independent of the specific distribution and is instead one of a point mass at the center of this sphere. In combination with Newton's second law of motion

$$\mathbf{F} = m\mathbf{a} \quad (8)$$

this allows us to calculate the speed of a star in circular orbit around the center of a perfectly spherical galaxy by setting the acceleration due to gravity equal to the centrifugal acceleration:

$$\begin{aligned} a_c &= \frac{v^2}{r} \\ a_g &= \frac{GM(r)}{r^2} \\ \Rightarrow v &= \sqrt{\frac{GM(r)}{r}} \end{aligned} \quad (9)$$

where  $r$  is the circular radius and  $M(r)$  is the mass of the galaxy enclosed within that radius.

Of course in reality, galaxies are not perfectly spherical. Most are either ellipsoids or disks, for the latter of which this is certainly not the case.

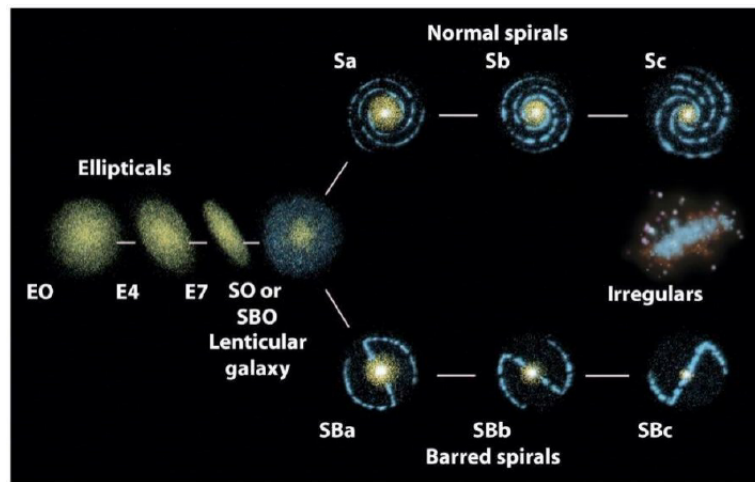


**Fig. 2:** Hubble classification of galaxies. Taken from <https://www.spacetelescope.org/static/archives/images/screen/heic9902o.jpg>

Since ellipticals are *dynamically hot*, the rotational speed of their gas can usually not

be assumed to be an indicator of the gravitational potential. But disks are *dynamically cold* and we do get information about the mass in the galaxy through their rotation curves.

Despite the non-sphericity of real galaxies, formula (9) provides a good approximation, especially because the dark matter halo of a galaxy, which in  $\Lambda$ CDM is the principal contributor to the total mass of the galaxy, is highly spherical.

The calculation can also be made more precise by using potential theory for thin disks, which gives quite similar results:

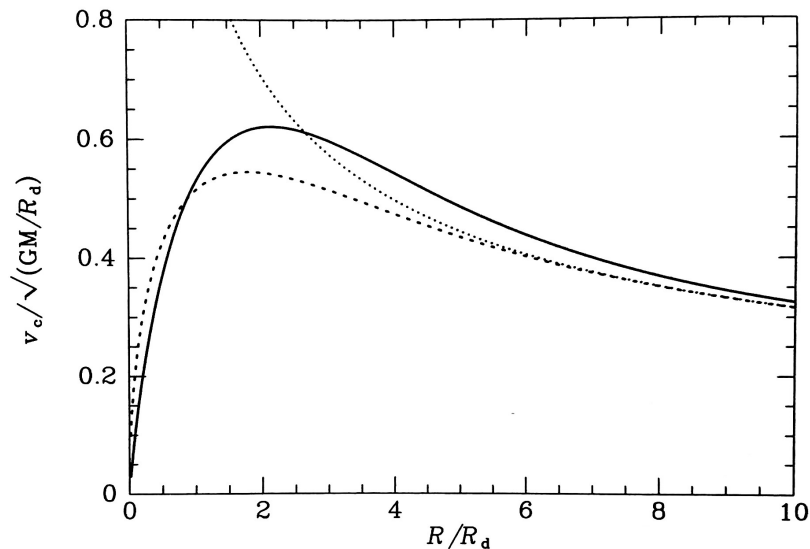


**Fig. 3:** Comparison of rotation curves, full curve: Exponential disk, meaning the surface density declines exponentially with radius. Dotted curve: Point mass with the total mass of the exponential disk. Dashed curve: Spherical distribution that has the same mass within a radius as the exponential disk.  $R_d$  is the exponential scale radius. Taken from Galactic Dynamics p.102.

Potential theory in combination with mass distributions of galaxies gained from luminosity observations predicts first a steep increase in the velocity and then a drop  $\sim \frac{1}{\sqrt{r}}$  ('Keplerian drop') for most galaxies.

As already mentioned, the latter part is not what is observed via Doppler-shift-spectroscopy of stars and gas of actual galaxies.

Rotation curves are usually measured by fitting a **Tilted Ring Model (TRM)** to a sky-map of line-of-sight-velocities (component of velocity parallel to line of sight). A TRM is constructed by finding a best fit for the velocity map of the galaxy by splitting it up into rings and varying inclination, position angle and rotation speed for each. The center of the galaxy in sky-coordinates is also allowed to vary and the procedure is per-

formed iteratively to get better and better agreement<sup>11</sup>.

Now instead of a Keplerian drop, the rotation curves appear flat far from the galactic center:

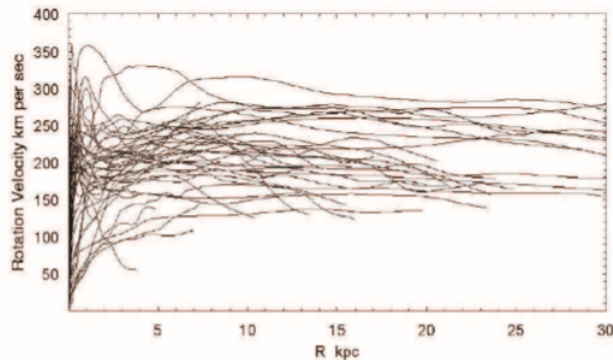


**Fig. 4:** Rotation curves of spiral galaxies. Taken from [Sofue and Rubin (2001)].

## 2.3 Dark matter halos

In  $\Lambda$ CDM, the flat asymptotic velocities in galaxies are explained by the presence of dark matter halos. A typical form for the density of a halo is the **Navarro-Frenk-White (NFW)** profile<sup>12</sup>:

$$\rho(r) = \frac{\rho_0}{\frac{r}{r_s} \left(1 + \frac{r}{r_s}\right)^2} \quad (10)$$

Here,  $r_s$  is a scale radius and  $\rho_0$ , as can be seen from the formula above, is four times the density at  $r = r_s$ . This can be integrated to obtain the total mass within a radius  $r$ :

$$M(r) = \int_0^r 4\pi s^2 \rho(s) ds = 4\pi \rho_0 r_s^3 \left[ \ln\left(\frac{r_s + r}{r_s}\right) - \frac{r}{r_s + r} \right]$$

Actually, the parameters  $\rho_0$  and  $r_s$  are thought to be closely correlated, with the NFW halos essentially having just one parameter, the **concentration parameter c** [Navarro et al. (1996)].

<sup>11</sup>The procedure was first described in Kornelis Begeman's 1987 PhD thesis available under <https://www.rug.nl/research/portal/files/2841681/thesis.pdf>. Page 14 of this PDF scan, page 15 of the original document.

<sup>12</sup>Galactic Dynamics p. 70

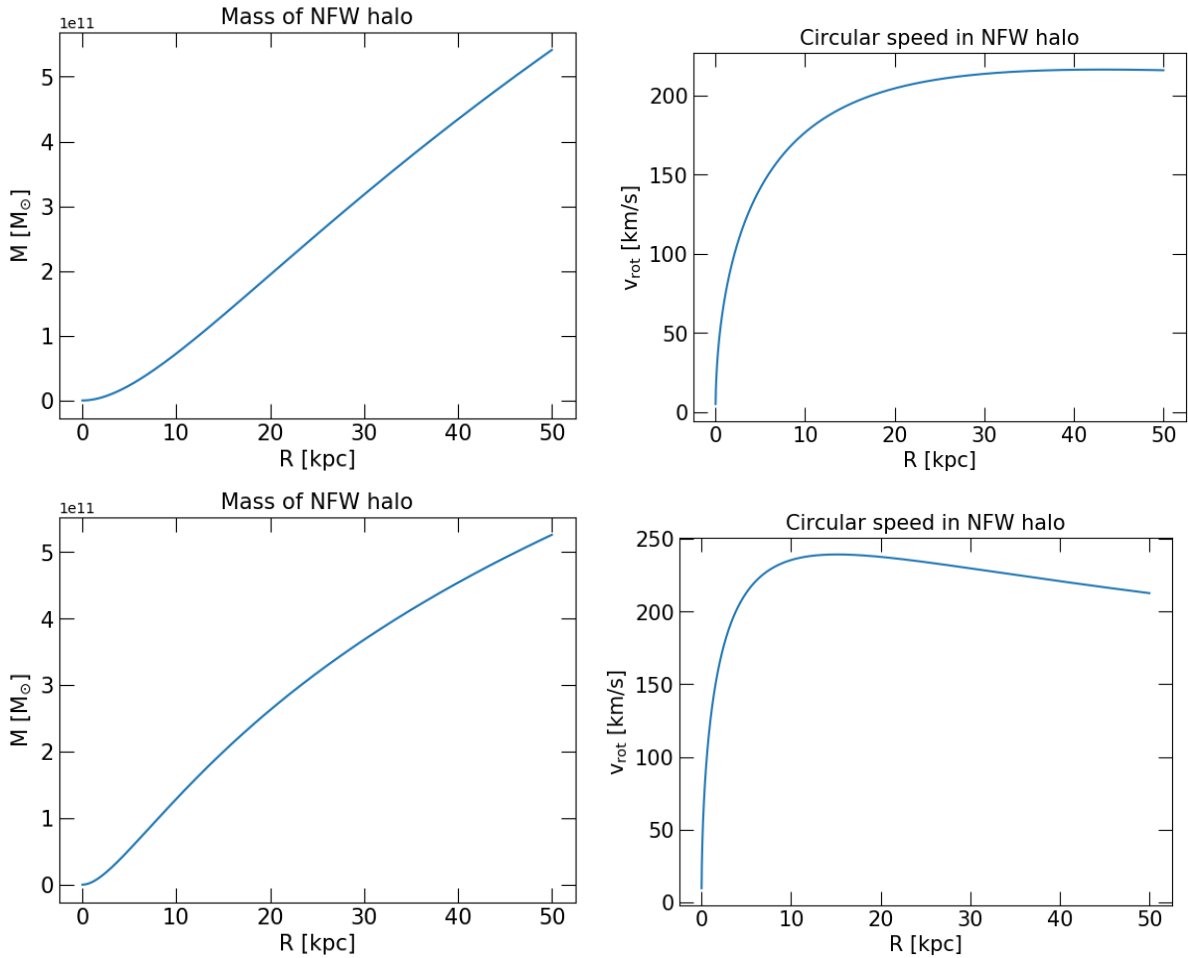


**Fig. 5:** NFW mass and speed profile (only DM considered!) Top:  $\rho_0 = 1 * 10^7 M_\odot/kpc^3, r_s = 20kpc$ . Bottom:  $\rho_0 = 1 * 10^8 M_\odot/kpc^3, r_s = 7kpc$ .

Cosmological simulations suggest that actual dark matter halos are more complicated and better approximated using an **Einasto profile**<sup>13</sup>:

$$\rho(r) = \rho_{-2} e^{-\frac{2}{\alpha}[(\frac{r}{r_{-2}})^{\alpha}-1]} \quad (11)$$

In contrast to the power-law form of the NFW, the intensity of curvature of the slope in the Einasto profile is determined by the additional parameter  $\alpha$ .

A fit to observations shows  $0.12 < \alpha < 0.25$  approximately and that  $\alpha$  increases with higher galaxy mass.

<sup>13</sup>Galaxy Formation and Evolution p.354

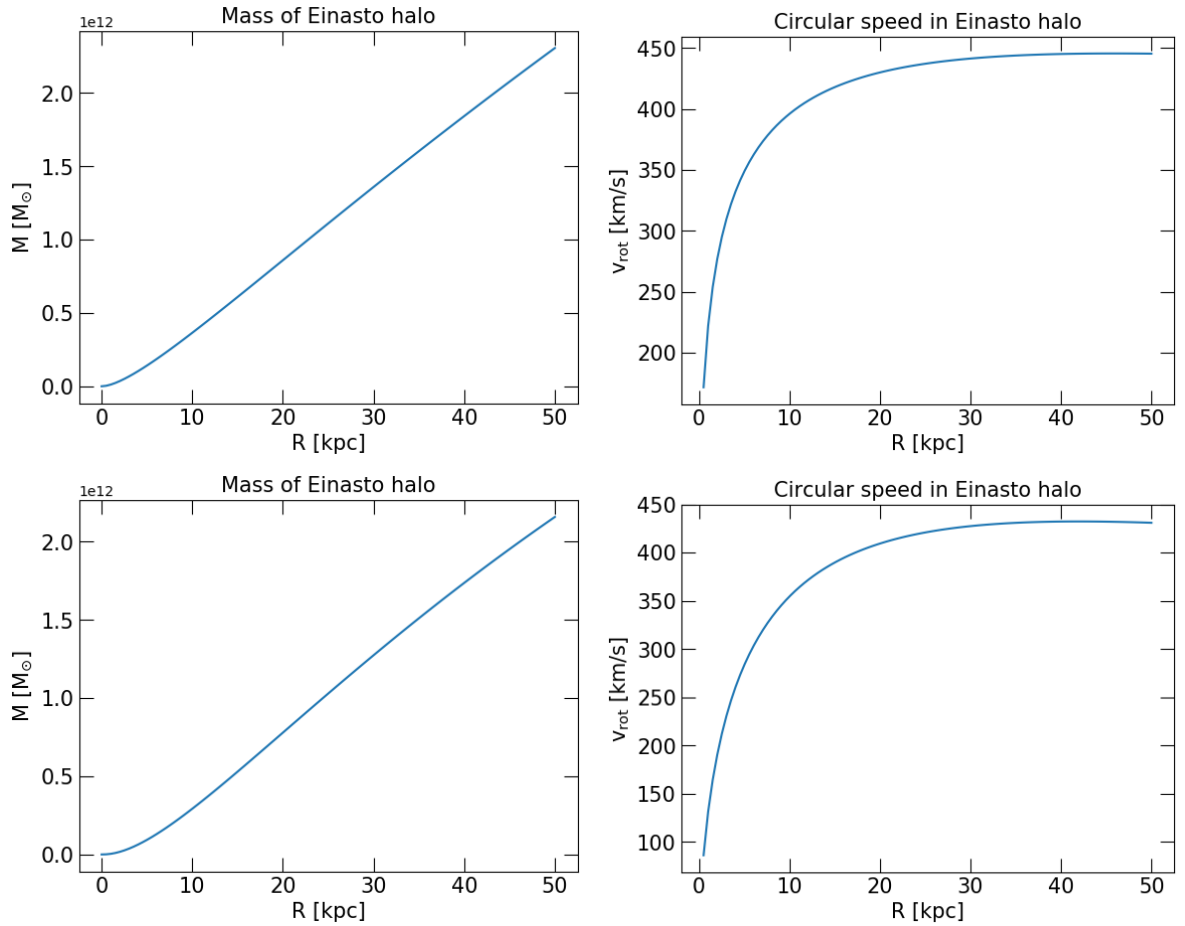


**Fig. 6:** Profiles of Einasto halo for  $\rho_{-2} = 1 \cdot 10^7 M_{\odot}/kpc^3$  and  $r_{-2} = 20kpc$ . Top:  $\alpha=0.12$ . Bottom:  $\alpha=0.25$ . The differences are very small, but for example observe that the speed profile at the top has a higher maximum.

## 2.4 Modified Newtonian Dynamics

In Modified Newtonian Dynamics, there is no such thing as dark matter. Instead, either equation (7) (which would mean MOND applies to gravitational forces only) or (8) (which would mean it applies to any force) is modified, hence the name.

Mordehai Milgrom, dissatisfied with what he saw as too many assumptions in the dark matter idea, proposed a different explanation for asymptotically flat rotation curves in 1983 [Milgrom (1983a), Milgrom (1983b), Milgrom (1983c)]: A modification at low accelerations, like those present in the outer regions of galaxies.

The new force law as a modification of equation (8) takes the form:

$$\mathbf{F} = m\mu\left(\frac{|\mathbf{a}|}{a_0}\right)\mathbf{a} \quad (12)$$

Or, expressed differently (and looking at magnitudes only):

$$\frac{a}{a_{new}} = \frac{1}{\mu\left(\frac{a}{a_0}\right)} \quad (13)$$

Here  $a_0$  denotes the characteristic acceleration scale, usually taken to be  $\sim 1.2 * 10^{-10} \frac{m}{s^2}$  [McGaugh et al. (2016)].

Milgrom explained in his original paper that he arrived at the new force law by supposing that at low accelerations, the force of inertia is no longer linearly proportional to the acceleration, while still retaining the assumptions that it is linearly proportional to mass, local and in the direction of acceleration. The  $\mu$  in equation (12) is the so-called *interpolation function*, which, while not entirely specified by MOND, is subject to two requirements:

a) At high accelerations, (12) should reproduce Newton's second law, equation (8). Therefore:

$$\mu(x) \rightarrow 1, x \ll 1$$

b) At low accelerations, (12) should reproduce the flat rotation curves observed at large radii/low accelerations. Therefore:

$$\mu(x) \rightarrow x, x \gg 1$$

Condition b) gives, in the limit of low accelerations (looking only at the radial component):

$$F = m \frac{a^2}{a_0} \quad (14)$$

Combining this with the centrifugal acceleration and (7) now yields:

$$\begin{aligned} \frac{GM(r)}{r^2} &= \frac{v^4}{a_0 r^2} \\ \Rightarrow v &= \sqrt[4]{Ga_0 M(r)} \end{aligned} \quad (15)$$

Here  $M(r)$ , in contrast to before, is only baryonic mass.

Equation (15) is a form of the **Tully-Fisher-Relation (TFR)**, which links the asymptotic rotation velocity (where the rotation curve is flat) and the total luminosity of a galaxy [Tully and Fisher (1977)]. The luminosity can then be linked to stellar mass using an appropriate Mass-to-Light ratio.

The luminosity form of this relation was known at the time of formulation and was therefore a central requirement MOND would have to meet. This scaling with **mass** is referred to as the **baryonic** Tully-Fisher-Relation [McGaugh and Schombert (2015)]. When I use the term TFR in this thesis, it refers to a scaling of asymptotic velocity with mass, not luminosity. The correlation with mass is the prediction by MOND and

in simulations we are fortunate enough to know the mass of every particle.

Attempts to change (7) by adding a radius dependence to obtain flat rotation curves at large radii were doomed to fail from the start because of the observed TFR [Sanders and McGaugh (2002)]:

A modification as a function of radius would take the form

$$F = \frac{GM}{r^2} f\left(\frac{r}{r_0}\right) \quad (16)$$

with a function of radius  $f$  and a radius scale  $r_0$ . To get asymptotically flat rotation curves, one would need  $f(x) \sim x$  at large radii. But this would lead to  $v^2 \sim M$ , in contrast to the TFR.

The specific rotation curves predicted by MOND can differ quite substantially depending on the interpolation function used, which will become apparent in the study of Magneticum galaxies later. Common choices and the corresponding relations between MONDian and Newtonian accelerations are [Dutton et al. (2019)]:

$$\begin{aligned} \mu(x) &= \frac{x}{1+x} \text{ 'Simple interpolation function'} \\ a_{MOND}(r) &= a_{new}(r) \left( \frac{1}{2} + \frac{1}{2} \sqrt{1 + 4 \frac{a_0}{a_{new}}} \right) \end{aligned} \quad (17)$$

$$\begin{aligned} \mu(x) &= \frac{x}{\sqrt{1+x^2}} \text{ 'Standard interpolation function'} \\ a_{MOND}(r) &= a_{new}(r) \sqrt{\frac{1}{2} + \frac{1}{2} \sqrt{1 + 4 \frac{a_0^2}{a_{new}^2}}} \end{aligned} \quad (18)$$

Or, alternatively:

$$a_{MOND}(r) = \frac{a_{new}(r)}{\nu\left(\frac{a_{new}(r)}{a_0}\right)} \quad (19)$$

$$\nu(y) = 1 - e^{-\sqrt{y}}$$

*From [McGaugh et al. (2016)], henceforth referred to as 'McGaugh interpolation function'.*

Of course in principle, infinitely many interpolation functions are possible - they just need to fulfill the basic requirements laid out above -, but I will stick to these three exclusively over the course of this thesis, with a focus on the McGaugh and simple functions. The McGaugh function is what I consider to be the most modern form of the MOND force-law. But for simplicity, I will often use the simple function instead, as the two give very similar results anyway, as we will see later.

The MOND law as it is stated above can merely be an empirical relation that follows from a more complete theory [Sanders and McGaugh (2002)]: If the modification (13) is simply applied to the Newtonian acceleration-vectors in every direction

$$\mu\left(\frac{|\mathbf{a}|}{a_0}\right) * \mathbf{a} = \mathbf{a}_{new},$$

then MOND suffers from serious theoretical problems, especially the violation of the laws of conservation of energy and momentum.

There are candidates for a complete theory of MOND which do not violate these conservation laws due to them being derived from a Lagrangian with the appropriate symmetries. The first of these was the so-called **Bekenstein-Milgrom theory** with the Lagrangian for the potential:

$$L = \rho\Phi + \frac{a_0^2 F\left(\frac{|\nabla\Phi|^2}{a_0^2}\right)}{8\pi G} \quad (20)$$

Here  $F$  is a suitable function, meaning one that ensures the MOND force-law follows in situations of high symmetry.

Following the usual Lagrangian formalism, assuming stationary action leads to:

$$\nabla \cdot \left[ \mu\left(\frac{|\nabla\Phi|}{a_0}\right) \nabla\Phi \right] = 4\pi G\rho \quad (21)$$

for  $\mu(x) = \frac{dF(x^2)}{dx}$ .

Basically, this is a generalization of Poisson's equation, which we get for  $\mu = 1$ . The equation of motion for a particle is the usual  $m\mathbf{a} = -\nabla\Phi$  - the dependence on acceleration is transferred to the potential in this theory.

A consequence of this formulation is the **external field effect**, which has become a central part of the MOND paradigm. This effect entails that the internal dynamics of a subsystem are affected by the external accelerations acting on the system as a whole. Milgrom already discussed one important situation in his original paper: Open clusters in galaxies do not show clear mass discrepancies, although their internal accelerations are very low. This problem is solved by noticing that the gravitational acceleration from the galaxy on the star cluster is actually much higher than the critical value  $a_0$ , turning the dynamics of the star cluster Newtonian.

The strong equivalence principle of general relativity is therefore violated with this formulation of MOND and a system cannot be decoupled from its environment. But observations strongly disfavor MOND without an external field effect [Pittordis and Sutherland (2019)].

There are also relativistic generalizations of MOND, among those **Tensor-Vector-Scalar-Gravity (TeVeS)** [Bekenstein (2004)]. Such a generalization is important, since gravitational lensing is often used to detect 'missing mass' and any non-relativistic theory of MOND shares the problem of Newtonian gravity when it comes to lensing: It

underpredicts the angle of deflection by a factor of 2. In the limit of strong fields, the relativistic MOND should reduce to general relativity.

As I stated in the introduction, there is no complete MOND-cosmology on the level of the  $\Lambda$ CDM model yet. But there are ideas, see for example [Kiselev and Timofeev (2012)].

In [Sanders and McGaugh (2002)], some probable basic points of a future MOND cosmology are laid out: First off, the Big Bang will almost certainly be part of this cosmology. Concerning matter in the universe, there is expected to be non-luminous baryonic matter, but no or at most negligible cold DM, although neutrinos as **hot** DM are expected to play a role. More specifics, including the prediction of early Reionization and even some cosmological simulations with MOND are discussed in [McGaugh (2014)].

Next, we will examine very distinct predictions made by MOND.

## 2.5 Acceleration relations

Under MOND, the observed flattening of rotation curves is not due to the presence of an as yet unknown form of matter, but instead is a result of the low accelerations in the outer regions of galaxies. Therefore, the discrepancy between the acceleration expected from the baryons and the observed one should depend solely on the acceleration in a given region.

This discrepancy can be thought of as either missing mass or missing acceleration, leading to the **Mass-Discrepany-Acceleration-Relation (MDAR)** and **Rotational-Acceleration-Relation (RAR)**, respectively. The formulas for the RARs for different interpolation functions are given above in equations (17), (18) and (19).

Next, we find equations for the MDAR predicted by MOND:

$$a = \frac{GM_{dyn}}{r^2}, a_{bar} = \frac{GM_{bar}}{r^2}$$

$M_{dyn}$  is the mass that is measured through the rotational velocity/ acceleration, while  $M_{bar}$  is the one expected from the distribution of baryonic mass.

We get:

$$\frac{M_{dyn}}{M_{bar}} = \frac{a}{a_{bar}} = \frac{1}{\mu(\frac{a}{a_0})} \quad (22)$$

where (13) was used.

To get a value for  $M_{dyn}$  at a given radius  $r$  in a galaxy, one takes the speed  $v$  of the gas at that radius and reverses (9):

$$M_{dyn} = \frac{v^2 r}{G} \quad (23)$$

The total acceleration is simply  $a = \frac{v^2}{r}$ . Essentially, the two relations contain the same information: The dynamical mass is calculated from the rotational acceleration, so in the end both rely on measurements of velocity and distance to the center of the respective galaxy. Still, some trends are visible more clearly in one than in the other, which is why both of them will be used over the rest of the thesis.

In addition, values for  $a_{bar}$  are necessary. Therefore, there is a need for a mass model, gained from luminosity observations and MLRs which in turn are preferably from stellar population models.

The **SPARC** (Spitzer Photometry & Accurate Rotation Curves) data set [Lelli et al. (2016)] includes rotation curves and mass models of 175 galaxies. It has allowed precise investigation of the RAR and MDAR in galaxies [McGaugh et al. (2016)] and has been used as a point of comparison to simulations before [Dutton et al. (2019)]. I too will compare Magenticum data mainly to this data set in later sections.

The SPARC mass models are given for an MLR of  $\frac{M_{\odot}}{L_{\odot}} = 1$ , meaning a star with the sun's luminosity is assumed to also have the mass of the sun. Following [Dutton et al. (2019)], I used an MLR of 0.5 for the disk and 0.7 for the bulge - but this is expected to vary from galaxy to galaxy.

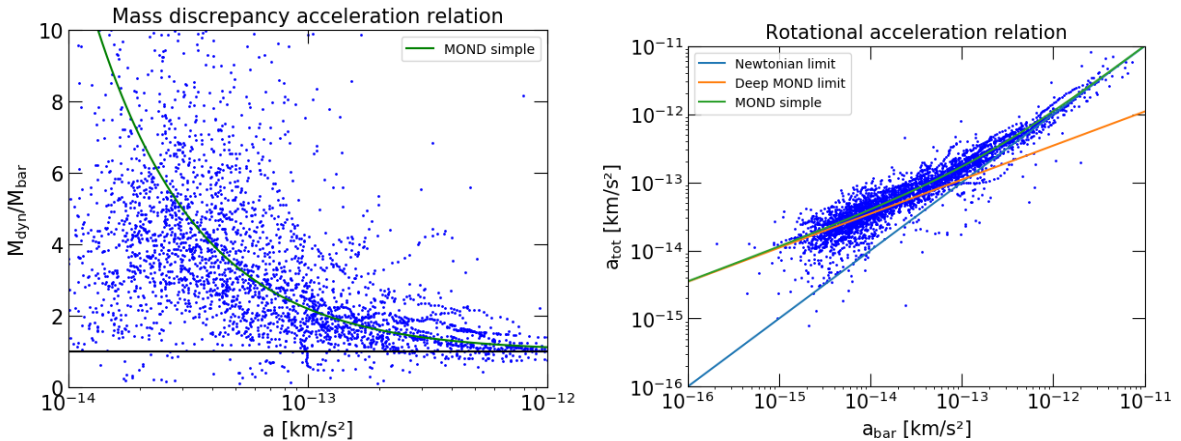


**Fig. 7:** MDAR and RAR in SPARC.

MOND does not allow for any intrinsic scatter in either of these relations. Any observed deviation from the RAR and MDAR must therefore be due to observational errors or incorrect models of galactic mass. [McGaugh (2014)] comes to the conclusion that the observational data is in fact consistent with a single force law.

On the other hand, if similar relations should also arise in the context of  $\Lambda$ CDM, i.e. in cosmological simulations, then intrinsic scatter and even systematic deviations are expected to exist [Navarro et al. (2017)].

## 2.6 The laws of galactic rotation

[McGaugh (2014)] summarizes the properties of galactic rotation curves I have discussed thus far as the following **laws of galactic rotation**:

- ”1. Rotation curves attain an approximately constant velocity that persists indefinitely (flat rotation curves).
2. The observed mass scales as the fourth power of the amplitude of the flat rotation (the Baryonic Tully-Fisher Relation).
3. There is a one-to-one correspondence between the radial force and the observed distribution of baryonic matter (the mass discrepancy acceleration relation).”

These are also the main properties I will be investigating in *Magneticum* over the course of this thesis.

While the first law was a piece of evidence that led to the idea of dark matter in the first place, it is not directly built into  $\Lambda$ CDM simulations. Instead, it naturally arises from dark matter being dissipationless and interacting through gravitation only, leading to the formation of halos.

The TFR for luminosity can be explained in a DM framework<sup>14</sup> by assuming the average surface brightness  $\langle I \rangle = \frac{L}{r^2}$  ( $L$  is luminosity) and the MLR (luminosity to *total mass* is meant here) to roughly be the same for all spiral galaxies. Solving (9) for the radius gives

$$L = \left(\frac{M}{L}\right)^{-2} \frac{1}{G^2 \langle I \rangle} v_{flat}^4. \quad (24)$$

The third one is clearly the most interesting. It is the most fundamental, as the other two laws can be derived from it. It also most specifically hints at MOND being an actual modification of dynamical laws.

The third law is often linked to **Renzo’s rule**, stated as [McGaugh (2014)]:  
 ”For any feature in the luminosity profile there is a corresponding feature in the rotation curve and vice versa.”

If this is indeed what is observed, then a-priori it seems to be more compatible with MOND:

In MOND, the rotation curve is determined almost exclusively by the position of stars in the galaxy (with some influence from gas), so luminosity and rotation speed are expected to be closely correlated. However, if dark matter dominates the mass of the galaxy and is distributed approximately spherically, then one can expect it to somewhat shield the influence of the baryons on the rotation curve. That is unless the dark matter follows the distribution of baryonic matter in a specific way that carries over these features, perhaps

<sup>14</sup>Explanation based on <http://www.usm.uni-muenchen.de/people/lesch/archiv/Vorlesung%20Galaktik%20und%20Extragalaktik/Vorlesung%202018/Vorlesung%204%20Welt%20der%20Galaxien.ppt>

as a result of the processes of galaxy formation.

As examples of where Renzo’s rule manifests itself, [McGaugh (2014)] points to dips in rotation curves

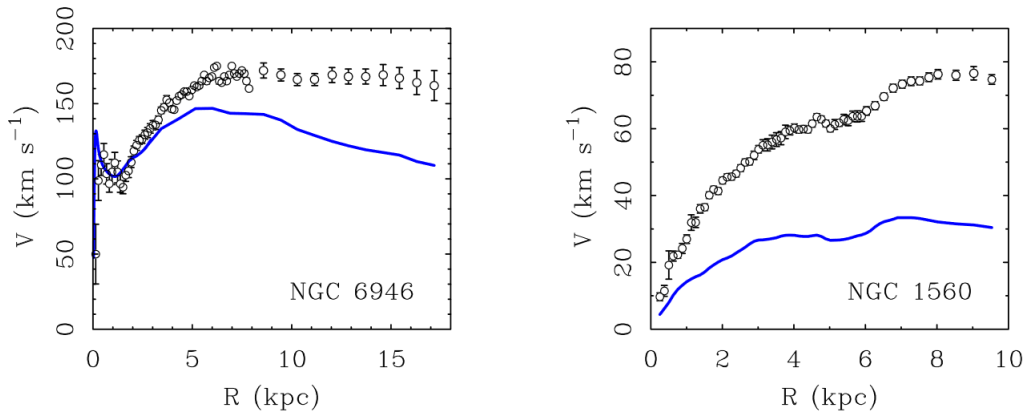


**Fig. 8:** Rotation curves of the galaxies NGC 6946 (left) and NGC 1560 (right) with their baryonic mass models in blue. Taken from [McGaugh (2014)].

and the observation that the curves of **high surface brightness (HSB)** galaxies (in this plot on the left) have a much steeper rise than the ones of **low surface brightness (LSB)** (on the right) galaxies.

The most noteworthy feature here is the dip in the right plot: In  $\Lambda$ CDM, the dynamics of this LSB galaxy are supposed to be dominated by DM, not the baryons. The question of how big the influence of baryons really should be is of course a central point of this thesis.

## 2.7 The Magneticum simulation

The Magneticum simulation is described in more detail in [Teklu et al. (2015)], but the basics will be paraphrased here.

The Magneticum pathfinder simulations are a set of cosmological hydrodynamical simulations performed with an extended version of the N-body/SPH code GADGET-3 (this set is what I call *the* Magneticum simulation, in singular). The predecessor GADGET-2 is described in [Springel (2005)]; updates include, among others, a different treatment of the viscosity [Dolag et al. (2005)].

The simulations include star formation with feedback and radiative cooling processes [Springel and Hernquist (2003)], which are very important to even get spiral galaxies. Chemical enrichment is treated as described in [Wiersma et al. (2009)]. Gas can be heated and metals produced through supernovae type Ia and II. Black holes and active galactic nuclei are simulated according to [Springel et al. (2005)], with the difference that in Magneticum, a gas particle can lose  $\frac{1}{4}$  of its mass to a black hole, so that it can

contribute up to four times to black hole accretion.

Of course initial conditions from the CMB are needed for the simulation, which in this case are taken from WMAP [Komatsu et al. (2011)]. The cosmological parameters of the used  $\Lambda$ CDM model are:  $h = 0.704$ ,  $\Omega_m = 0.272$ ,  $\Omega_\Lambda = 0.728$ ,  $\Omega_b = 0.0451$  and  $\sigma_8 = 0.809$ , where the first four parameters have the meaning explained above and  $\sigma_8$  is the present matter fluctuation averaged over a sphere of radius  $8h^{-1}$  Mpc.

The galaxies used in this thesis are all from box 4 of the Magneticum simulation and are at redshift  $z=0$ . For an in-depth description of the structure of the Magneticum disk galaxies, see [http://www.usm.lmu.de/CAST/student\\_projects/bachelor\\_theses/schulze\\_bachelor.pdf](http://www.usm.lmu.de/CAST/student_projects/bachelor_theses/schulze_bachelor.pdf).

As I have stated above, this thesis will instead focus on the **dynamics** of the Magneticum galaxies, and will especially examine the presence of the laws of galactic rotation in Magneticum.

### 3 MOND in Magneticum

Now I will discuss my findings in the Magneticum simulation. I begin with basic calculations of rotation curves, both theoretical and based on gas particles. These are compared to the predictions of MOND for Magneticum galaxies and the TFR. The RAR and MDAR in Magneticum data will be examined and then compared to SPARC data. 2D maps of gas and theoretical velocities are shown, followed by a refinement of predictions using potential theory, allowing me to investigate Renzo's Rule.

#### 3.1 Rotation curves of Magneticum galaxies

First, the simple formula (9) will be used to get a basic idea about the shape of theoretical rotation curves in Magneticum. 14 'poster child'-galaxies were predominately used here, which were pre-selected.

Let us first take a look at theoretical rotation curves with only baryonic matter considered in comparison to the ones with dark matter.

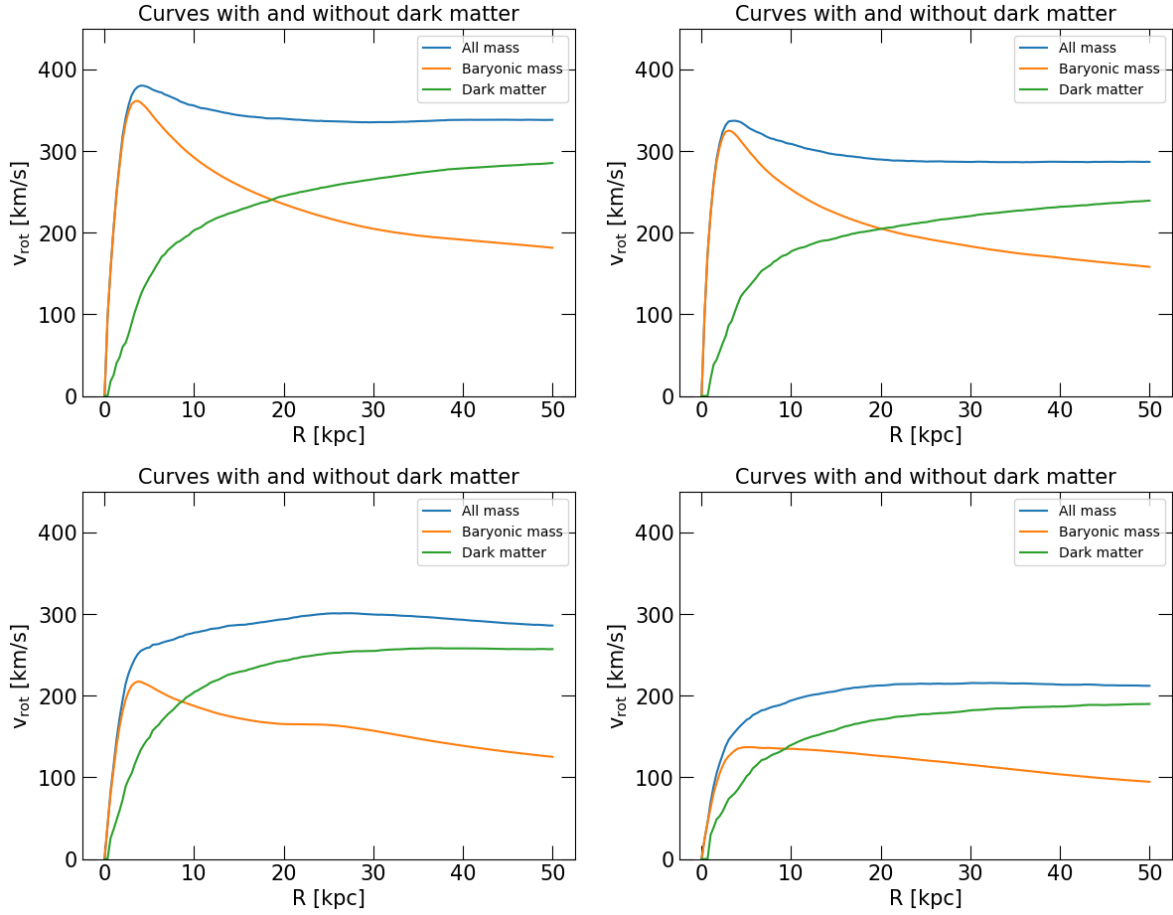


**Fig. 9:** Rotation curves with and without DM. From top left to bottom right: 28,36,105,172.

The baryonic curves are quite similar to the one gained from potential theory in figure 3, showing first a steep increase and then a Keplerian drop-off. The curves with dark matter usually start to strongly deviate at about the peak of the baryonic velocity prediction. I have chosen the galaxies above to reflect the different 'types' of curves - while some show first a 'hump' and then a drop to a flat asymptotic velocity, others reach the asymptotic velocity at the peak of the baryonic velocity and others again even show an increase of rotation speed in the outer regions.

Another interesting thing to look at is the difference between the MOND predictions for different interpolation functions. The curves were calculated using the formulas (17), (18) and (19) above.

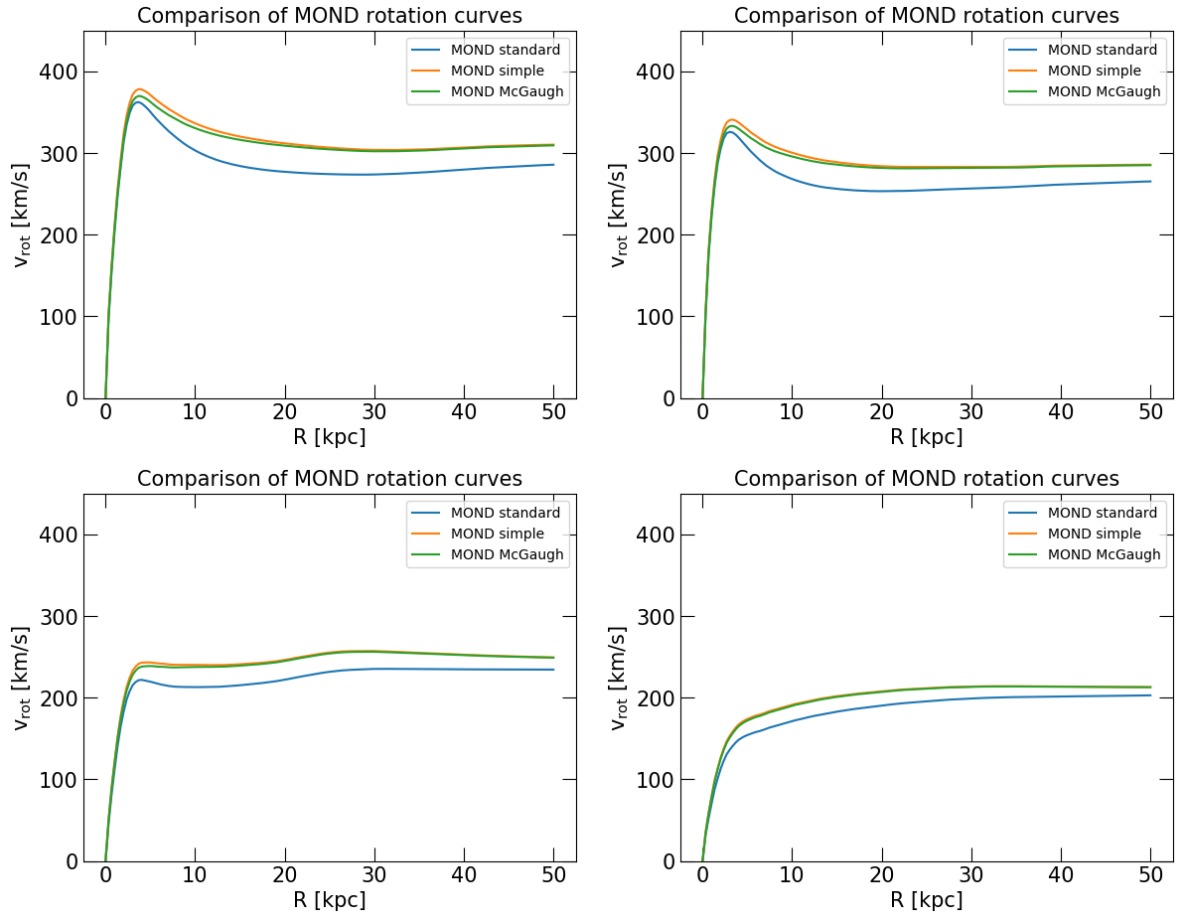


**Fig. 10:** MOND rotation curves. From top left to bottom right: 28,36,105,172.

One can see that, as I have already stated above, the simple and McGaugh curves are quite similar, while the standard curve only reaches the other two farther out, meaning at even lower accelerations.

The next focus will be on the differences between dark matter and MOND predictions:

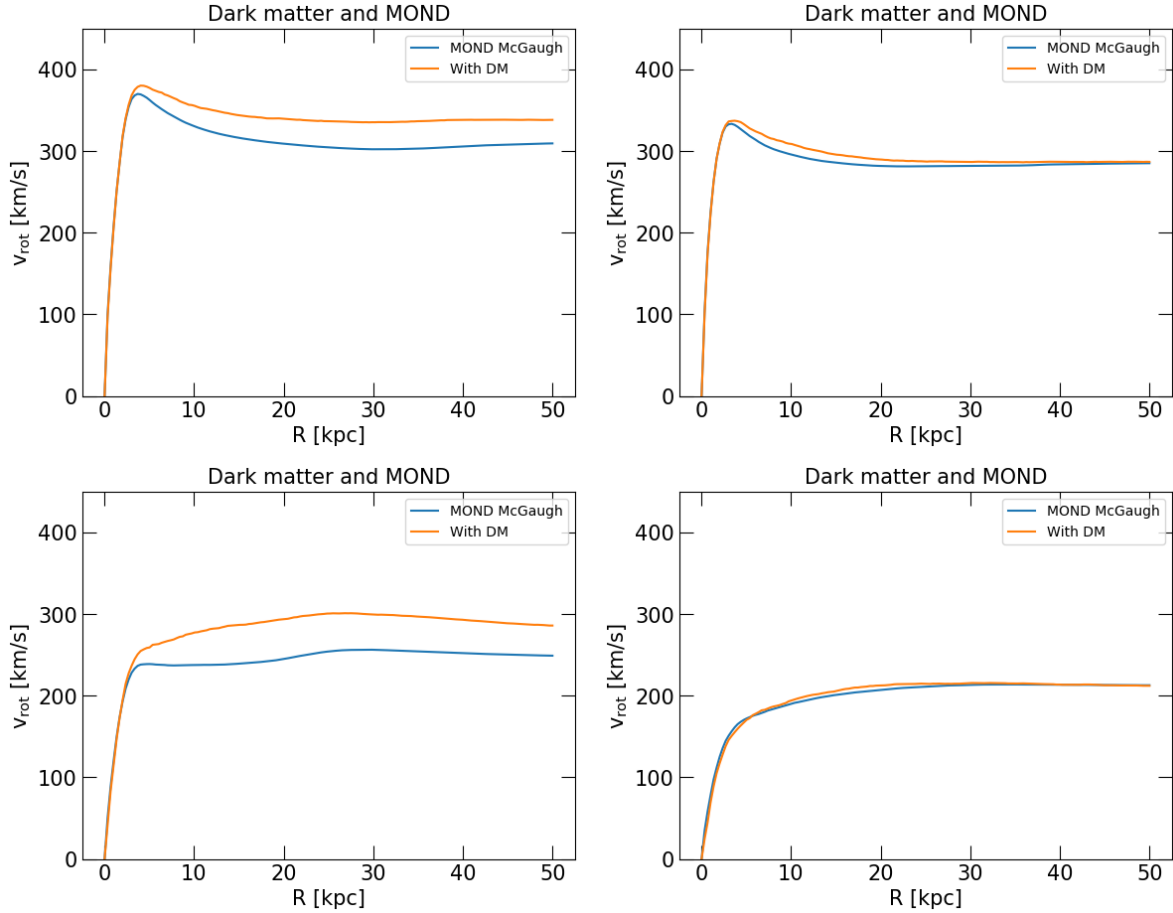


**Fig. 11:** DM and MOND. From top left to bottom right: 28,36,105,172.

Both the dark DM and MOND curves show flat asymptotic velocities in accordance with the first law of galactic rotation. But some DM curves (see appendix) actually show a slight decline at larger radii, which is not possible under MOND (in regions of low acceleration!).

Both curves clearly differ from the Newtonian curve without DM. While some of the MOND predictions are very similar to the 'actual' curves based on DM, sometimes the differences are great, mainly in the form of substantially higher and lower asymptotic velocities. The more pronounced presence of certain 'bumps' in MOND curves are another distinguishing feature. Since the rotation curve in MOND depends solely on baryons, this is not surprising.

Up to this point all curves were based on what the rotational speed of the gas at a certain radius *should be*, not on what it *actually is*. Therefore it is time to see how the gas particles actually behave in Magneticum galaxies.

For this, the velocities were projected onto the unit vector tangential to a circular orbit (the positive direction is anti-clockwise when viewed from above, but the absolute values

are taken after averaging anyway):

$$\mathbf{k} = \hat{z} \times \mathbf{r} \quad (25)$$

$$v_{rot} = \mathbf{v} \cdot \mathbf{k}$$

$\hat{z}$  is the unit vector in z-direction and  $\mathbf{r}$  and  $\mathbf{v}$  are the position and velocity vector of the gas particle, respectively.

A weighting mechanism was used to extract rotation curves: Instead of using 'hard' bins where a particle is either fully contained in a certain radial bin or not, particles further away from the radius associated with a bin contribute less when taking the average of the velocities in that bin. The used weighting scheme is essentially equivalent to the *Particle in cell* mass assignment, in, for example, some cosmological simulations:

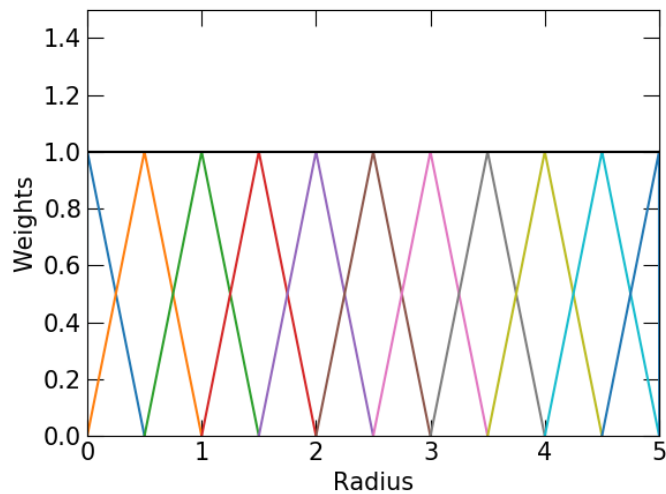


**Fig. 12:** Gas weighting. Different colors show different radial bins. The weights add to 1 everywhere as is necessary to preserve the center of mass.

This means that there are twice as many particles in one radial bin as with 'hard' bins of the same radial spacing - some particles just contribute less.

I excluded the inner 5 kiloparsec of each galaxy, as these regions are dominated by non-circular motions of the gas and are therefore not a good tracer of the gravitational potential. Also, only the cold gas ( $T < 10^5 \text{K}$  or  $\text{coldfrac} > 0$ , the latter means the particle is 'hot' solely for numerical reasons) was used, because the hot gas can in general not be assumed to be in circular motion either. Lastly, we are interested in the dynamics of the disks, so only particles with  $z < 3 \text{kpc}$  and  $z > -3 \text{kpc}$  were counted.

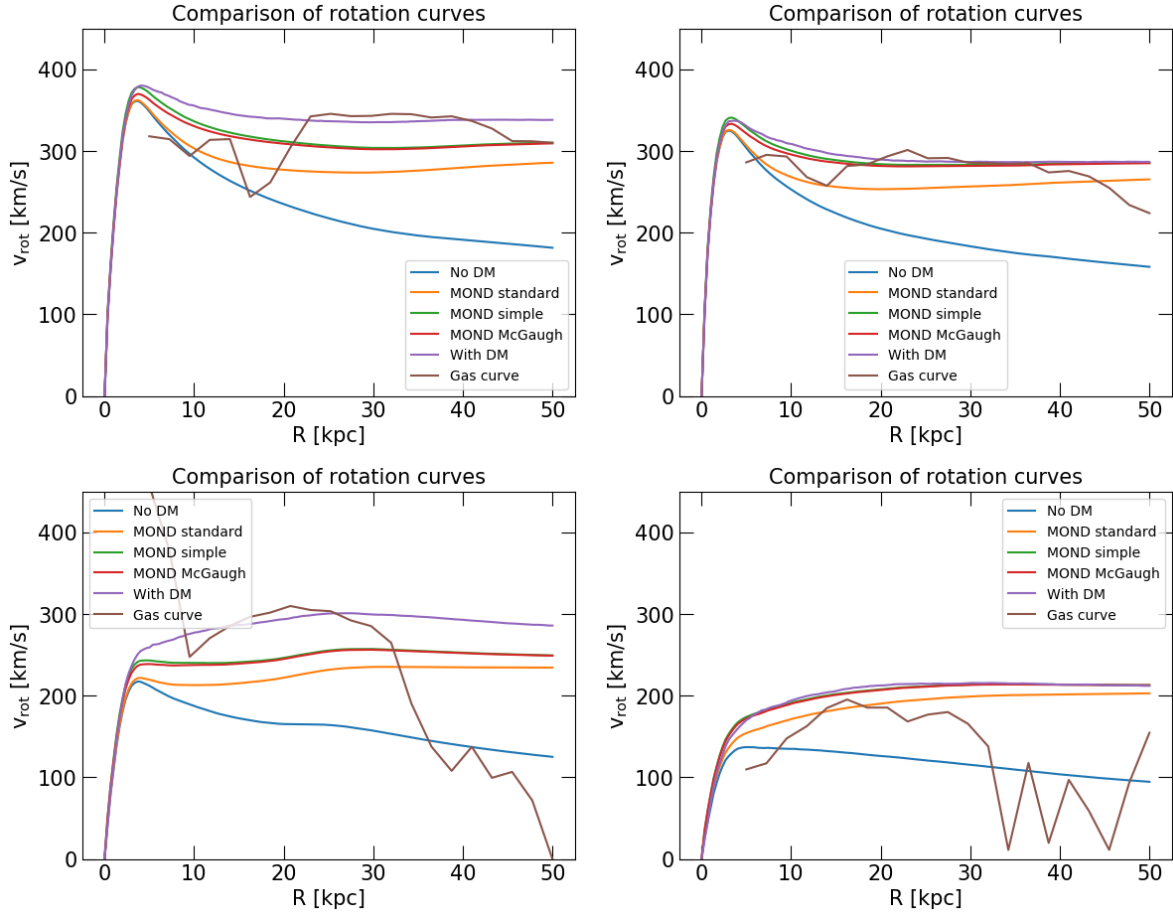


**Fig. 13:** Including gas. From top left to bottom right: 28,36,105,172.

(Curves of the other galaxies can be found in the appendix.)

The gas of some galaxies is significantly slower than expected theoretically. This will become a problem later when trying to get a meaningful RAR and MDAR from the Magneticum data. I will however show there that the data points which most strongly deviate from expectations are the result of bins including very few particles. This mainly happens in the outer regions of galaxies, but occasionally the inner ones can also be quite gas-free. This is sometimes a result of excessively strong AGN-feedback in Magneticum and will be clearly visible as rings of gas in the 2D maps we will study at a later point.

Because of the recurring problems with the gas as a tracer for the gravitational potential, I decided to mainly use the theoretical values calculated from the DM distribution as a way to get a Magneticum TFR, RAR and MDAR. Admittedly, using the gas would be preferable, but the problems with the gas are clear here. If  $\Lambda$ CDM actually can reproduce MOND relations, then this would necessarily be due to a certain DM halo structure. In reality, there is much more gas and it can reasonably be assumed to follow the gravitational potential more closely. Therefore, the fact that gas in Magneticum does not actually follow the distribution of DM as closely as expected should not pre-

vent us from getting meaningful results from the fundamental properties of Magneticum galaxies, meaning the mass distributions.

### 3.2 TFR in Magneticum

The next step is the second law of galactic rotation: The asymptotic velocity of a galaxy scales with the fourth power of the total baryonic mass. Asymptotic means within a radius of  $\frac{1}{8}r_{vir}$  here and the total baryonic mass is also assumed to be contained in a sphere with that radius. Due to the almost complete absence of gas this far out, I used the total mass along with (9) to get the asymptotic velocity.

More galaxies than the 14 posterchilds are needed to actually get a meaningful relation. Therefore, I used all of the Magneticum galaxies with a **b-value** of  $b > -4.375$ . The b-value is a measure of how much the galaxy is rotation- as opposed to pressure-supported, based on specific angular momentum. As a reminder: Pressure-supported galaxies, i.e. ellipticals are dynamically hot, which is why in observations, the speed of their gas can not be reliably treated as a measure of the potential. So the rotation-supported galaxies (high b-value) are what we are interested in.

Using these 152 galaxies, we can fit a TFR to the data and compare it to the relation predicted by MOND, 15. The fitting function has the form  $f(M) = (aM)^b$ .

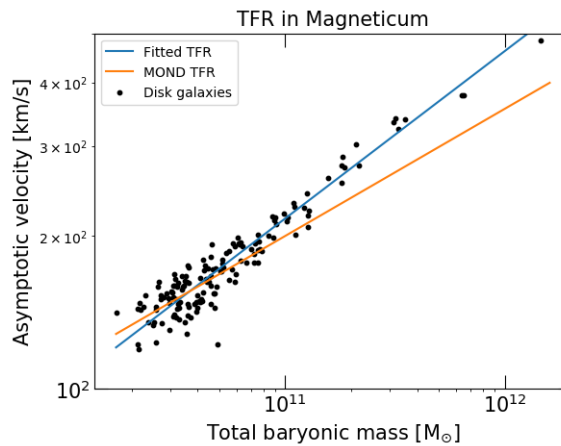


**Fig. 14:** Tully-Fisher-Relation.

The parameters of the fitting function are  $a \approx 1.24 * 10^{-4} (km/s)^{1/b} / M_{\odot}$ ,  $b \approx 0.33$ . MOND, in the form of (15), predicts  $b = 0.25$ ,  $a = G * a_0 \approx 1.59 * 10^{-2} (km/s)^4$ .

There is a strong deviation in regions of higher mass. But spiral galaxies in nature rarely show masses above  $\sim 10^{11} M_{\odot}$ . The high mass disks in this plot should not be disks at all - and they are not. These are ellipticals which have high b-values due to their extended gas disks.

By excluding galaxies above this threshold, we get a different picture:

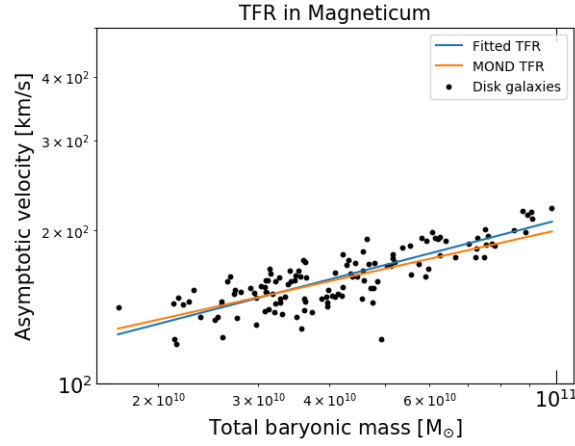


**Fig. 15:** TFR, excluding high masses.

The parameters are now  $a \approx 1.02 * 10^{-3} (km/s)^{1/b} / M_{\odot}$ ,  $b \approx 0.29$ . There is the possibility that MOND would not actually predict the exponent 4 for the chosen galaxies and radii: If the accelerations are still in the intermediate regime, then the exponent will be different. To test this, I calculated the MOND velocities from the total baryonic mass enclosed at the cut-off radius by the same method as the MOND rotation curves before. Here there is of course only one value for each galaxy. Then I again fitted a TFR, comparing it to the usual MOND parameters given above:

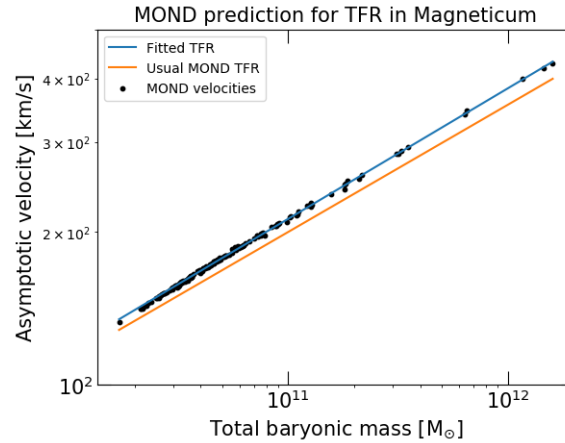


**Fig. 16:** MOND TFR for galaxies in Magneticum.

This gives  $b \approx 0.26$ .

The accelerations at the maximum radius seem to actually be in a range where the velocity should scale with the fourth power of the baryonic mass (the lines are almost parallel), so this cannot explain the discrepancy.

It should be mentioned that  $\frac{1}{8}r_{vir}$  is usually already very far out. A point of comparison: According to [Bland-Hawthorn and Gerhard (2016)], the virial radius of the Milky

Way is  $r_{vir} = 282 \pm 30 kpc$ , which means  $\frac{1}{8}r_{vir} \approx 35 kpc$ . But according to the same source, data is really only available out to  $r \approx 23 kpc$ .

Having checked this, the exact radius used does not appear to make a difference, as long as the rotation curve is actually flat in that region. So this also does not seem to be the cause for the differences between MOND and Magneticum in the baryonic TFR.

Therefore the discrepancy is unlikely to just be the result of a kind of bias, but more likely to be an actual difference between MOND and Magneticum predictions.

### 3.3 MDAR and RAR in Magneticum

The next step are the MDAR and RAR in Magneticum and investigating whether the third law of galactic rotation is reproduced. For this, I again used all galaxies with b-values  $> -4.375$ , with 15 points from each galaxy, evenly spaced between  $\frac{1}{200}r_{vir}$  and  $\frac{1}{10}r_{vir}$ , for a total of  $2280 = 15 \cdot 152$  data points.

I first used the gas of these galaxies, but as it was to be expected from the rotation curves, it gave generally low values for the acceleration. To investigate whether these outliers are part of smaller bins than the others, I colored the data points according to their bin size:

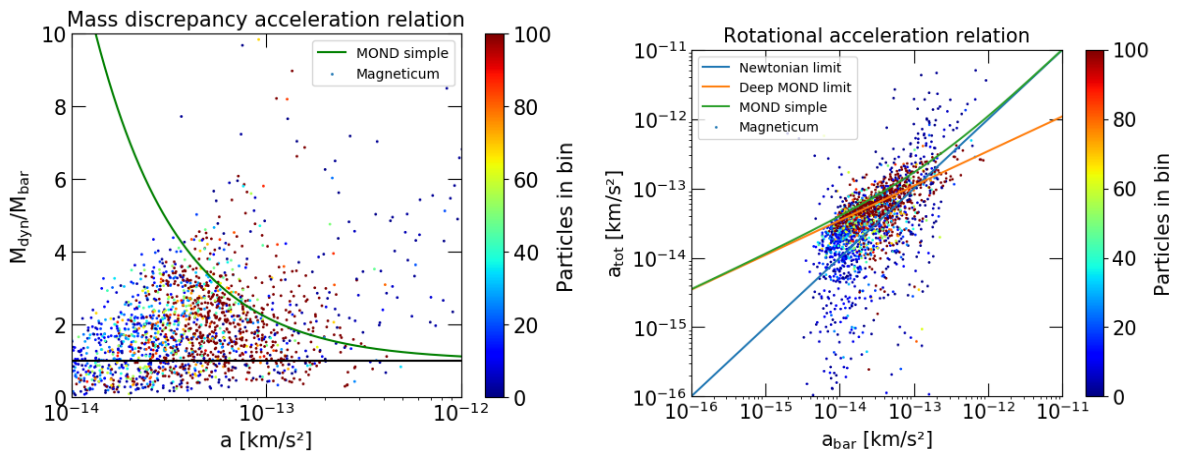


**Fig. 17:** Magneticum gas.

The points which are closest to the lower left corner are mostly from small bins. Still, bigger bins also deviate strongly from the MOND (and SPARC) RAR and MDAR.

As I have already stated above, this prompted me to use the mass distributions directly instead of inferring it via gas velocity. From a  $\Lambda$ CDM standpoint,  $M_{dyn} = M_{bar} + M_{DM}$ . I used this together with (9) to get another RAR and MDAR, based not on dynamics, but on mass profiles. For this, the same galaxies and radii as for the gas were used.

Recalling the MDAR in MOND for a given interpolation function (22), we can see that the MDAR for the simple interpolation function has a distinct form:

$$\frac{M_{dyn}}{M_{bar}} = 1 + \frac{a_0}{a}$$

This lead me to use a function of the form  $f(a) = c_0 + \frac{c_1}{a} + \frac{c_2}{a^2} + \frac{c_3}{a^3}$  with parameters  $c_0, c_1, c_2, c_3$  to perform a least-squares fit to the Magneticum data. The result can be seen here, along with the RAR in Magneticum:

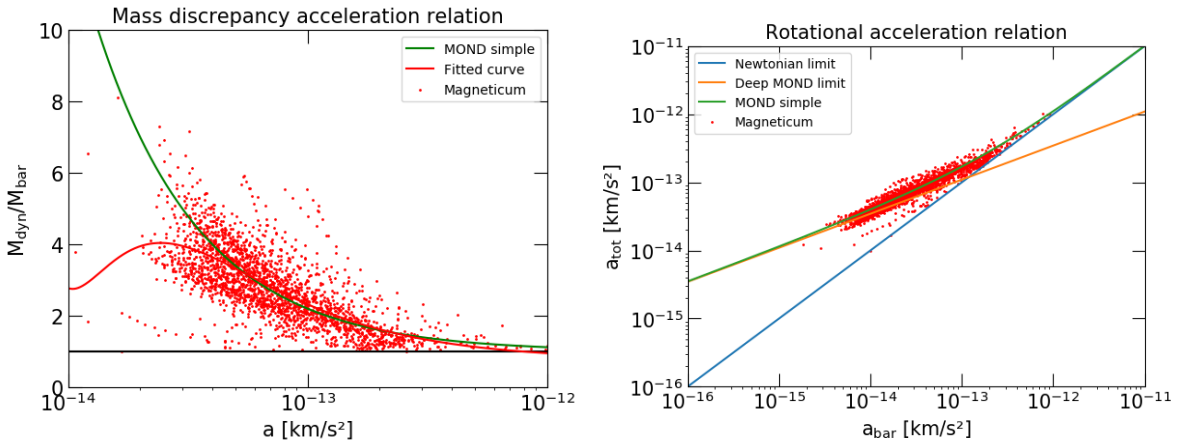


**Fig. 18:** Fitting MOND to Magneticum.

The parameters are  $c_0 \approx 0.77$ ,  $c_1 \approx 1.86 * 10^{-13} km/s^2$ ,  $c_2 \approx -3.24 * 10^{-27} km/s^2$ ,  $c_3 \approx 1.58 * 10^{-41} km/s^2$ .

The resulting curve deviates strongly in the regions of lower acceleration, but almost no data points are present there. In the region where most of the points lie, the differences between the MOND law and the MDAR in Magneticum are quite small.

Therefore, looking at galaxies from Magneticum, one could arrive at a force law similar to that of MOND.

This notion is reinforced by comparing the Magneticum data to SPARC:

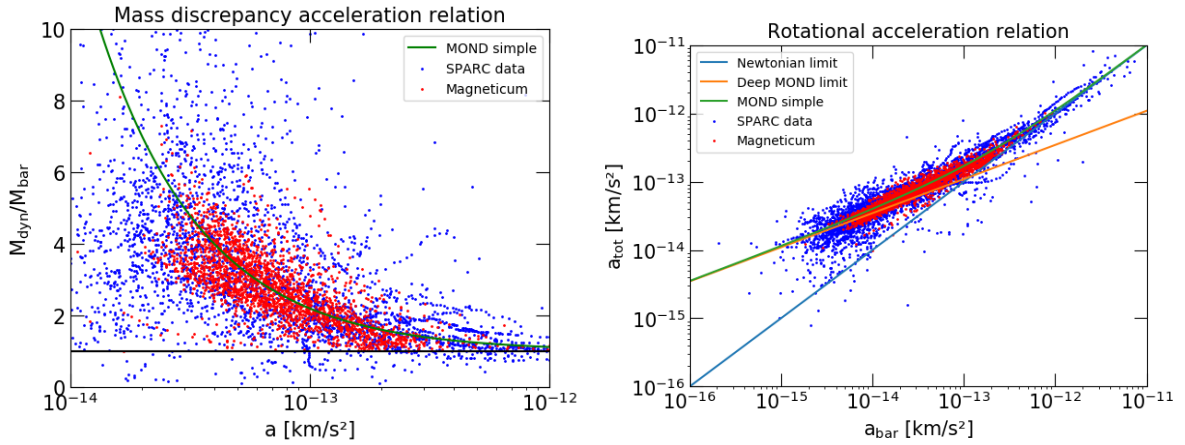


**Fig. 19:** Magneticum and SPARC.

One might expect there to be some correlation between the deviation of a galaxy from the MDAR/RAR and the  $b$ -value of that galaxy. But this does not seem to be the case:

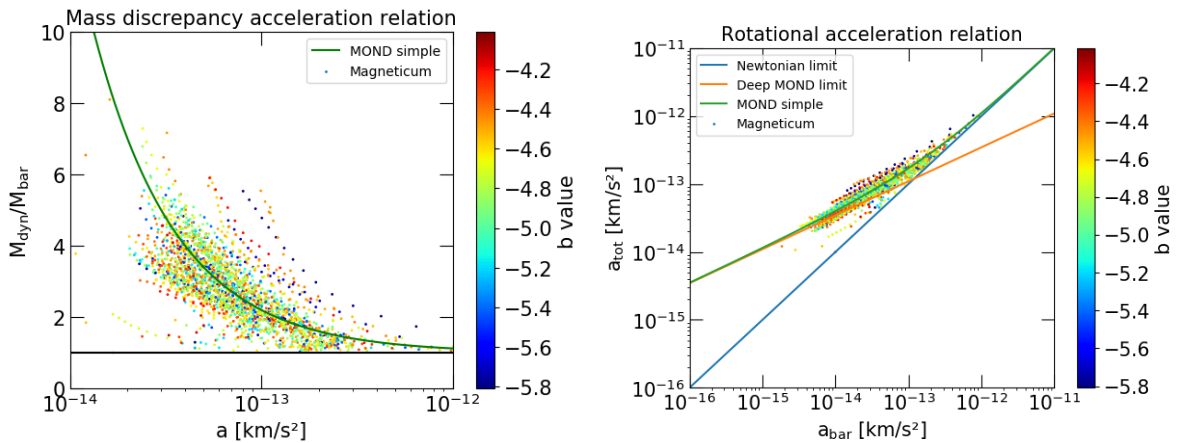


**Fig. 20:**  $b$ -values in RAR and MDAR.

The  $b$ -values appear to be rather evenly distributed over the respective plots. This plot allows us to see 'trails' formed by individual galaxies. The SPARC data also includes those, though primarily in the regions of higher acceleration and they generally seem to cover a narrower range of accelerations.

Of course they can be expected to be more dispersed in the SPARC data, as observational error and non-circular gas motion have to be considered in observations.

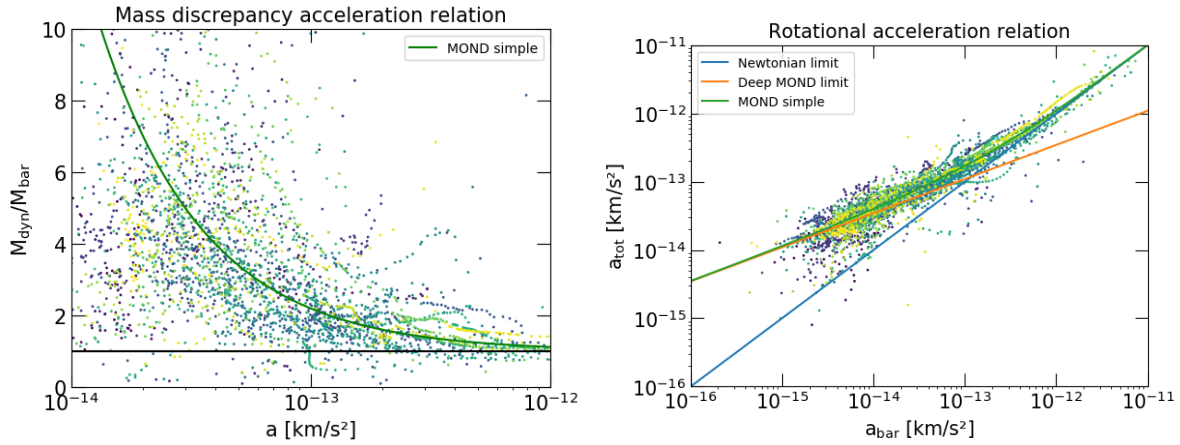


Fig. 21: Trails in SPARC data.

We can also look for a correlation with mass:

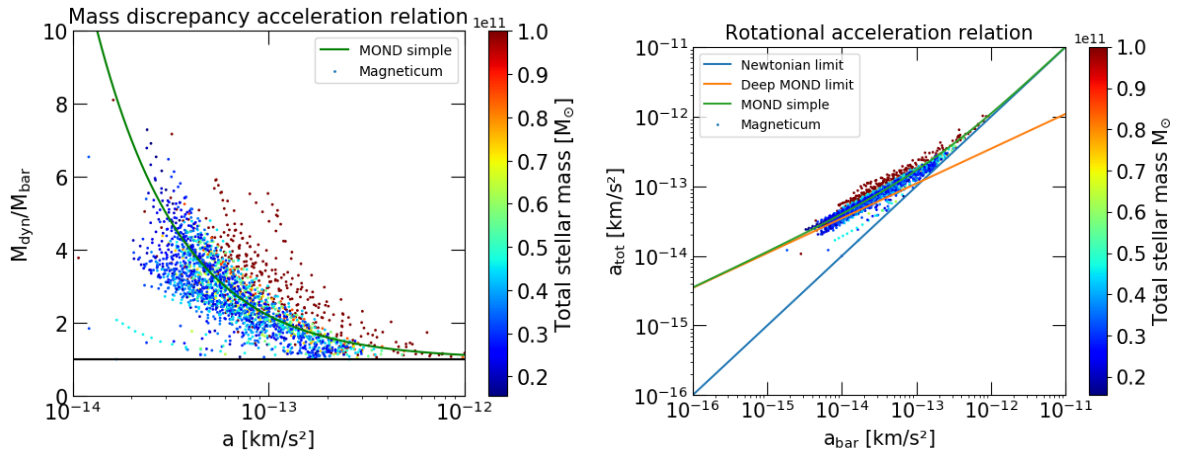


Fig. 22: MDAR and RAR with galaxy masses.

Galaxies that lie above the MOND MDAR generally have higher masses. Some of these actually have total stellar masses far above  $10^{11} M_{\odot}$ , signifying that those are the ellipticals with high b-value we encountered in the TFR.

But it seems that even among actual spirals, galaxies with high stellar mass tend to have higher ratios than MOND would predict.

### 3.4 2D maps of rotational velocity

The calculation of the rotation curves and the binning of gas particles until now do not contain any information about non-axisymmetric features. As a first step towards investigating how such features influence the dynamics of the galaxy, we can view the rotating gas in 2D instead of the 1D rotation curve:

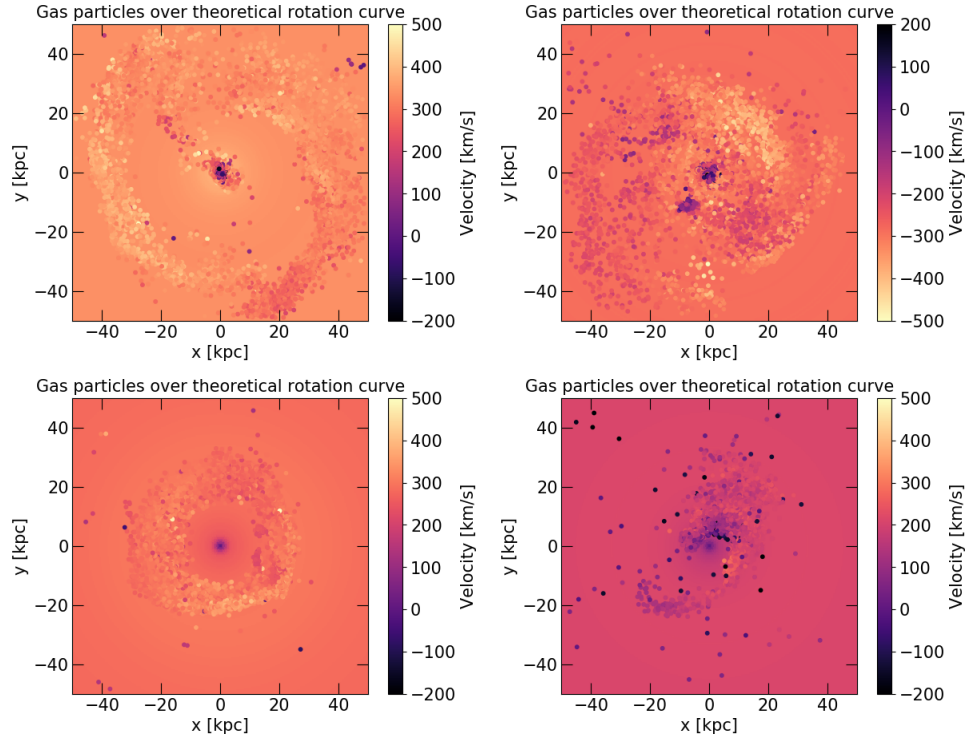


**Fig. 23:** Rotation maps for different galaxies. From top left to bottom right: 28,36,105,172.

(Maps for other galaxies in the appendix.)

Gas in a slice of  $\pm 5$  kpc height of the plane of galactic rotation is displayed here. The dots are gas particles, with their color indicating their rotational velocities. The calculation for theoretical values of the speed using (9) is shown in the background as color. At this point the theoretical calculation is still completely axisymmetric.

By inspecting the colorbar, it can be seen that there are galaxies rotating in both directions here when viewed from above, although I did invert the colorbar for the clockwise-rotating galaxies so that brighter always means faster. Essentially, points which appear brighter than the background are moving faster than predicted, while the ones which are darker move slower.

One of the aforementioned gas rings is visible in galaxy 105. There are also hints of spiral arms, most commonly in an 'S'-shape with two large arms (galaxies of this type are called '*grand design spirals*'). These arms additionally indicate the direction of rotation. Such local structures have a huge effect on the velocity of the gas, which is often collectively moving faster or slower than predicted in a spiral arm.

In reality, spiral arms are density waves<sup>15</sup> which move through stars and gas that are already present (although they often trigger star formation, which is why spiral arms appear blue). They are **not** composed of a fixed set of stars.

<sup>15</sup>Galactic Dynamics p.458 et sqq.

These figures exist mainly to get a better picture of how local structures manifest themselves in the Magneticum disk galaxies. The most valuable piece of information they provide is that a more accurate way to get theoretical rotation curves is needed. Such a method should also be able to capture non-axisymmetric features.

### 3.5 2D predictions of velocity from the gravitational potential

Up to this point, theoretical rotation curves were calculated using the simple approximation of a spherical distribution of matter, (9). To get more specific predictions, one can calculate the potential of the galaxy numerically and obtain a 2D map of the theoretical rotational velocity (in principle, the calculated map is actually 3D, but the rotational plane of the galaxy is what matters). This can be done by using the gravitational potential:

$$\mathbf{F} = -\nabla\Phi \quad (26)$$

$$\mathbf{F}(\mathbf{r}) = -G \int_{\mathbb{R}^3} d\mathbf{r}' \frac{\mathbf{r} - \mathbf{r}'}{|\mathbf{r} - \mathbf{r}'|^3} \rho(\mathbf{r}') \quad (27)$$

$$\Rightarrow \Delta\Phi = 4\pi G\rho \quad (28)$$

Here,  $\mathbf{F}$  and  $\Phi$  are the gravitational field and potential, respectively. Using the potential in combination with (8) allows us to calculate the rotational velocity:

$$\frac{v^2}{r} = -\frac{\partial\Phi}{\partial r} \quad (29)$$

A simple method to obtain the potential is via the **relaxation method**. In principle, it relies on the fact that solutions  $u$  of the Laplace equation

$$\Delta u = 0, \quad (30)$$

also called **harmonic functions**, have the **mean-value-property**. This property entails that (in 3 dimensions):

$$\forall r > 0 : u(x, y, z) = \frac{1}{\frac{4}{3}\pi r^3} \int_{B(x,y,z;r)} u dV \quad (31)$$

$B(x,y,z;r)$  is the ball of radius  $r$  around the point  $(x,y,z)$ . So numerically, the solution can be obtained by simply iteratively setting the value at a point equal to the average of the surrounding points. This can also readily be generalized to Poisson's equation

$$\Delta u = f, \quad (32)$$

where the value at a point has on 'offset' from the average value of the surrounding points, given by the value of  $f$  at that point multiplied by the grid-spacing  $h$  squared.

This follows from approximating the second derivative in a discrete way

$$\frac{d^2\Phi}{dx^2} \approx \frac{\Phi(x-h) - 2\Phi(x) + \Phi(x+h)}{h^2}$$

and solving for  $\Phi(x)$  (3D works out the same).

The solution of Poisson's equation requires specified boundary conditions, which are usually given in one of two forms:

- 1) **Dirichlet boundary conditions**, where the value of the function at the boundary is specified, or
- 2) **Neumann boundary conditions**, where instead the normal derivative of the function at the boundary of the domain is specified.

Dirichlet boundary conditions are usually simpler to implement by just holding the values at the boundary constant during the iteration. The problem is that the galaxies we want to look at are in empty space in an, for the purposes of this discussion, infinite universe. This leads to the boundary condition:

$$\Phi(r) \rightarrow 0, r \rightarrow \infty, \tag{33}$$

but we only want the potential in a region around the galaxy, because more space means more computation time and/or less resolution.

When one artificially forces the potential to 0 at a distance from the center of the galaxy where the potential should actually still be quite dominant, this leads to unrealistically steep gradients, which in turn, by (29), gives very high values for the rotation speed.

But a trick can be used: Far away from the galaxy, the potential approaches that of a pointmass with the mass of the galaxy positioned at the center of that galaxy:  $\Phi(r) = -\frac{GM}{r}$ .

This allows us to use the values of this approximate potential on the boundary of the box where the potential is calculated and use that as our Dirichlet conditions. This improves the results, but may not completely eliminate the associated problems, as we shall see.

First all of the particles, meaning their masses, need to be assigned to points of the grid. I simply assigned the mass of a particle to the grid point closest to it. There are obviously ways of doing the assignment that are numerically preferable (particle in cell would already be an improvement), but features on galactic scales are resolved quite well in this way - and with reasonable computational heaviness.

Similar to previous parts, the main concern is the interplay between dark and baryonic matter. Therefore I performed the relaxation with and without DM and derived a theoretical velocity field from both potentials individually, using (29). All of the following pictures show the galactic plane of a given galaxy.

I purposefully chose not to hold the colorbar constant for the following plots, as doing

so would make it very hard to see structures in the galaxies with lower mass: The total mass inside a sphere of radius 30 kpc ranges from  $3 * 10^{11} M_{\odot}$  to  $8 * 10^{11} M_{\odot}$ .

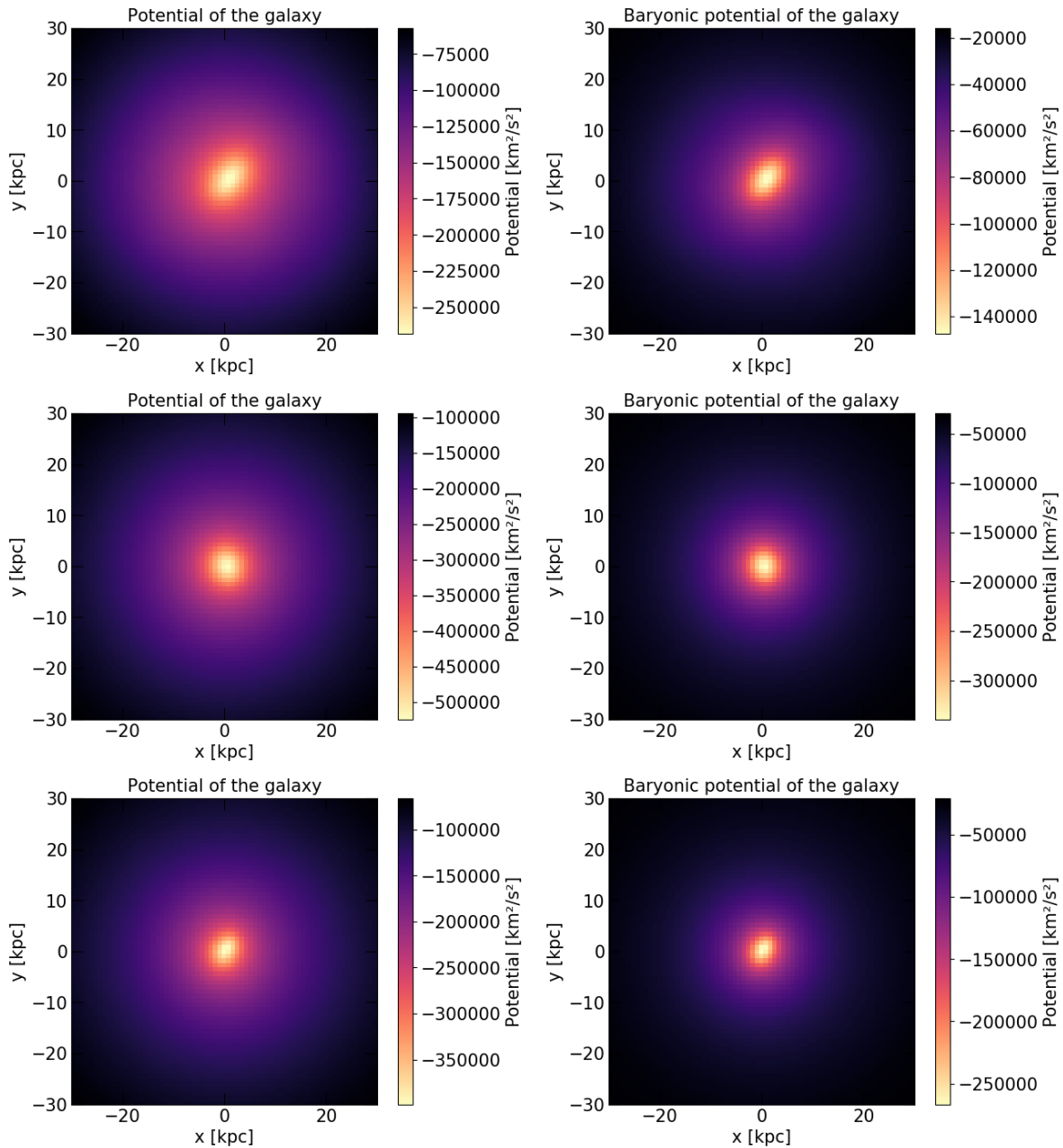


**Fig. 24:** Total and baryonic potentials of different galaxies. From top to bottom: 20,28,36.

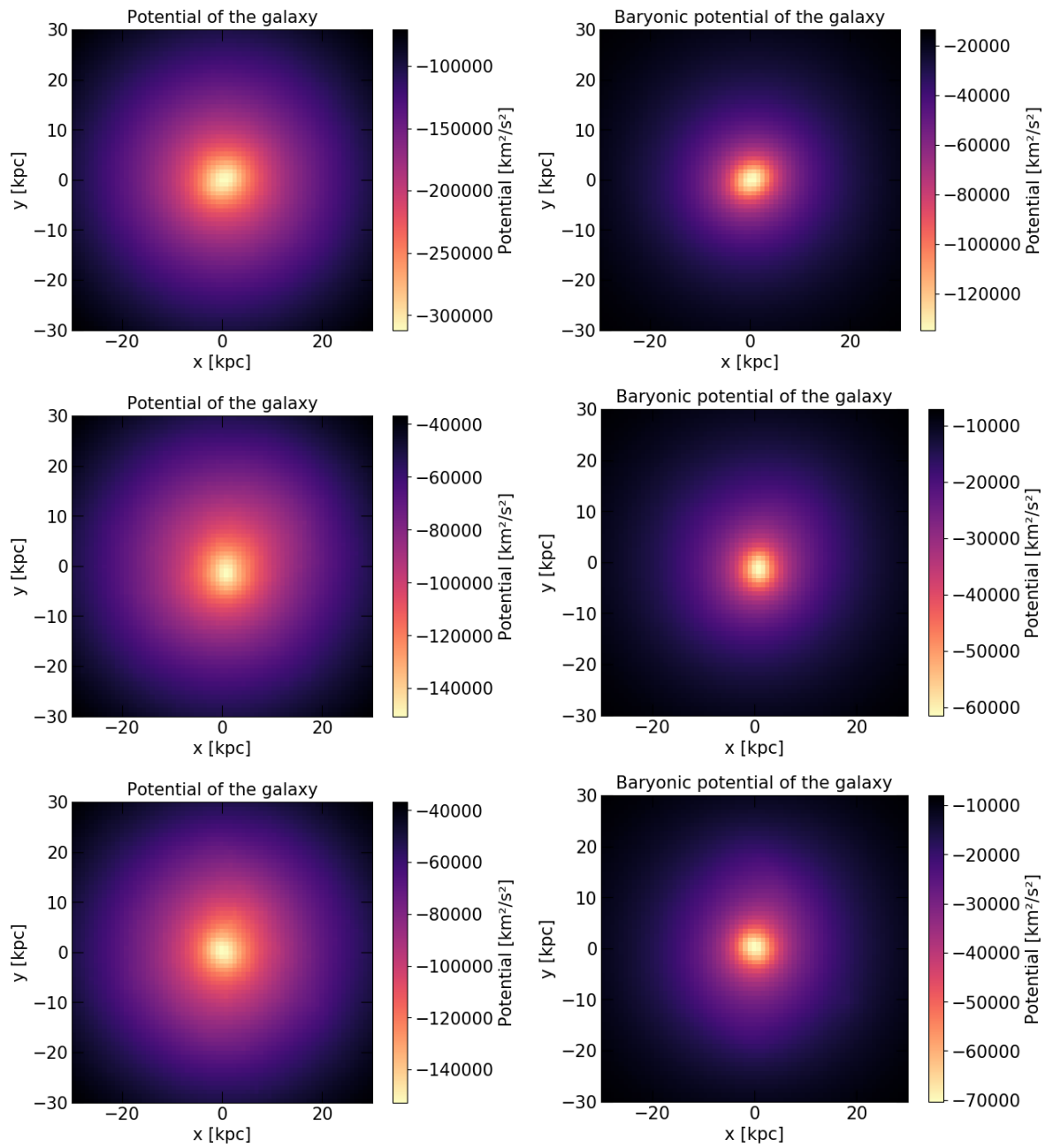


**Fig. 25:** Total and baryonic potentials of different galaxies. From top to bottom: 105,172,202.

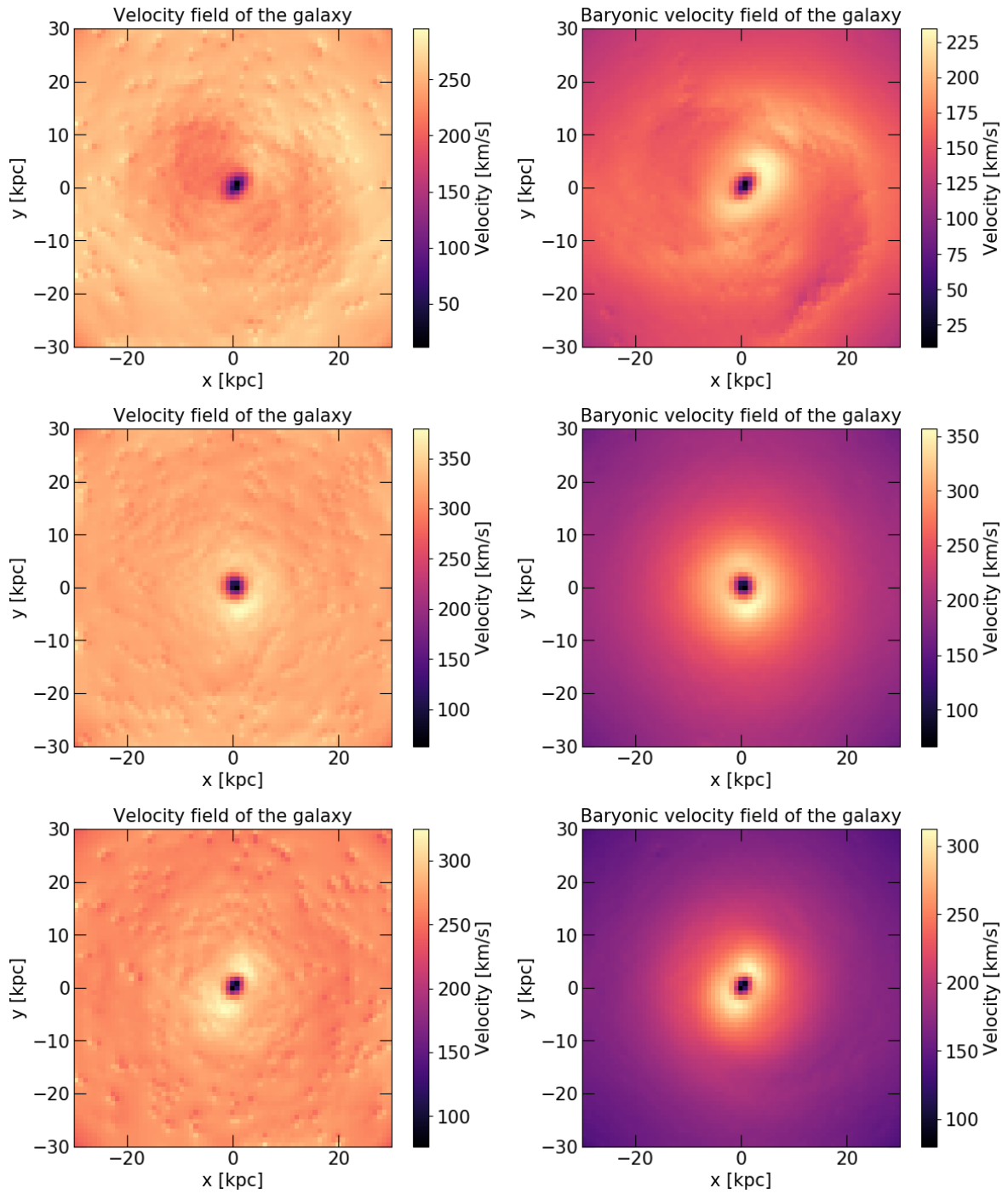


**Fig. 26:** Baryonic and total velocity fields of different galaxies. From top to bottom: 20,28,36.

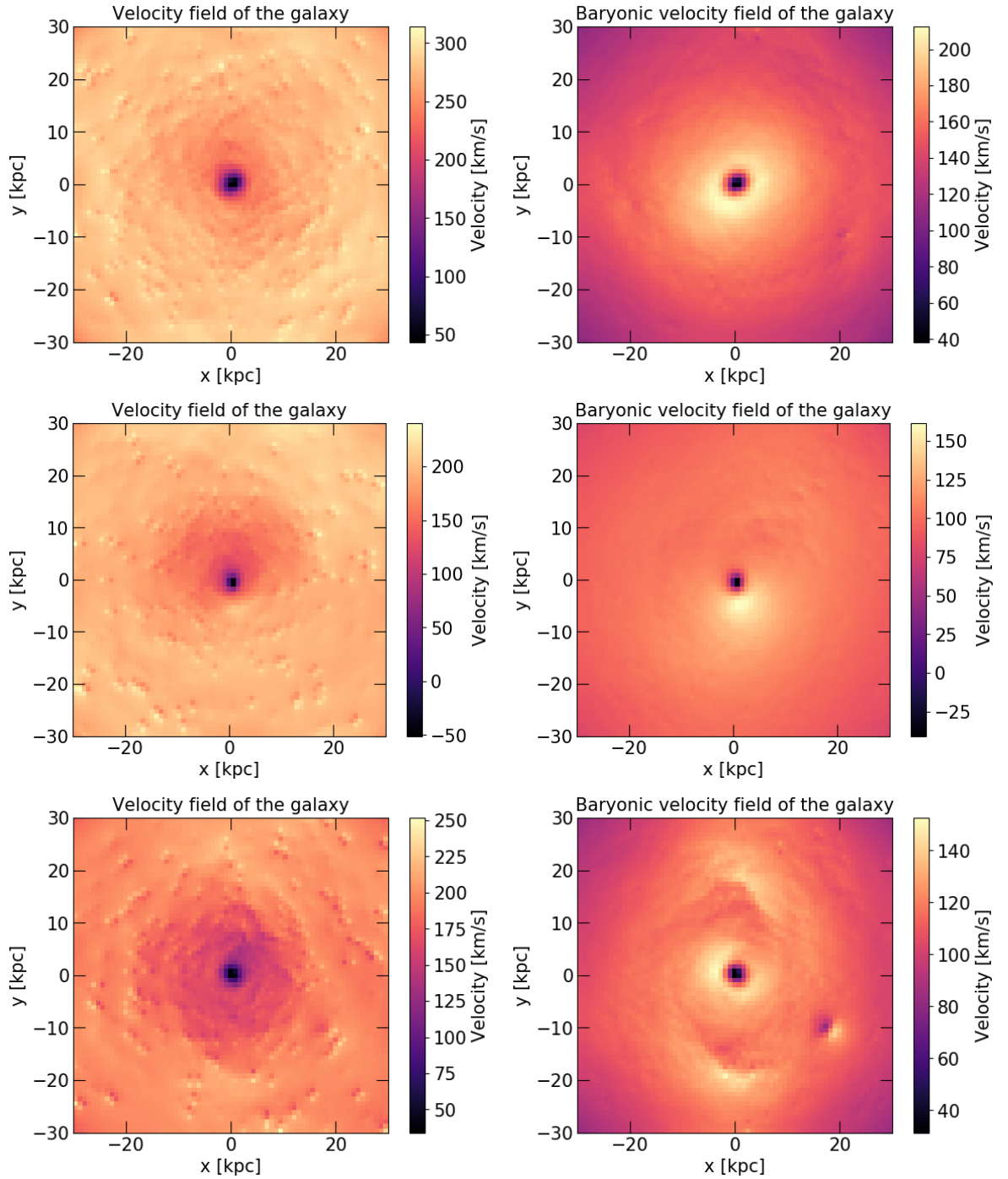


**Fig. 27:** Baryonic and total velocity fields of different galaxies. From top to bottom: 105,172,202.

Renzo's Rule manifests itself in the theoretical rotation curves: Features from the baryonic velocity prediction are carried over to the DM velocity field, although they appear somewhat less pronounced. This might also be affected by the choice of colormap, though. What really matters is whether these velocity fields follow the MDAR of MOND.

### 3.6 MDAR for individual galaxies

We can now take a closer look at the RAR and MDAR. The velocities and corresponding accelerations of every gridpoint can be used to obtain a RAR and MDAR for one galaxy.

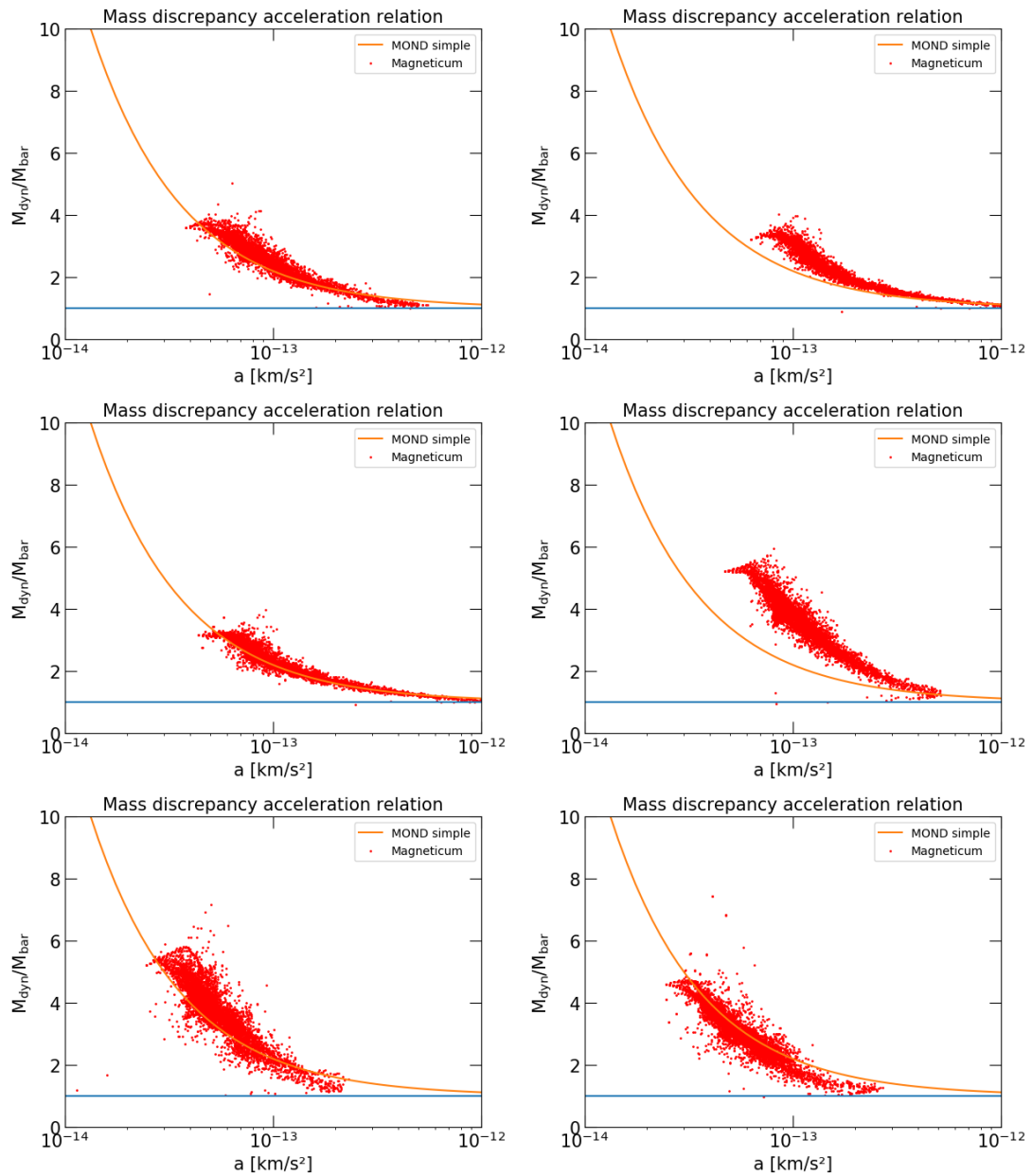


**Fig. 28:** MDARs of different individual galaxies. From top left to bottom: 20, 28, 36, 105, 172, 202.

(The remaining ones are in the appendix.)

The RAR and MDAR for the most part follow the trend predicted by MOND. Especially

the small scatter in galaxies 20 and 36 is remarkable.

The deviation from the MOND RAR seems to be greater in more massive galaxies. This might have a numerical origin: For bigger galaxies, we again encounter the problem of a large part of the halo lying outside the box in which the relaxation is performed. The effect on the slope of the gradients is also present in the baryonic velocity curve, but stronger in the curve with the total mass, which leads to the calculated MDAR and RAR of these galaxies being shifted to higher ratios of mass/acceleration discrepancy.

On the other hand, the velocities calculated in this manner are very close to the ones calculated in 1D before (figure 9, compare also to the appendix), signifying that this numerical problem might have a negligible effect. We have also already seen that more massive galaxies from Magneticum tend to have higher dynamical to baryonic mass ratios than predicted by MOND in general.

Convergence tests would need to be performed to fully rule out numerical errors here, which was not possible in the limited time for this bachelor thesis.

## 4 Mass models, dark matter halos and the MDAR

This section will look at the interplay of baryonic and dark matter in the context of the MDAR. First, mass profiles from Magneticum are discussed and compared to what MOND would predict for the halo. Then baryonic mass profiles are 'derived' from common halo shapes using the MOND MDAR. Next it is demonstrated how the MDAR changes with the parameters of a simple model of a spiral galaxy. Lastly, general results for the connection between DM halos and the MDAR are derived.

### 4.1 Mass profiles of Magneticum galaxies

The presence of MOND phenomenology in Magneticum must have its origin in the distribution of mass in its galaxies, which in turn is a result of the galaxy formation processes at play in universe a with DM.

We should therefore examine the mass profiles of individual Magneticum galaxies more closely. Given a baryonic matter profile, one can calculate the shape the DM halo would need to have to exactly mirror the effects of MOND. This is done by solving (22) for the total mass; I used the simple interpolation function.

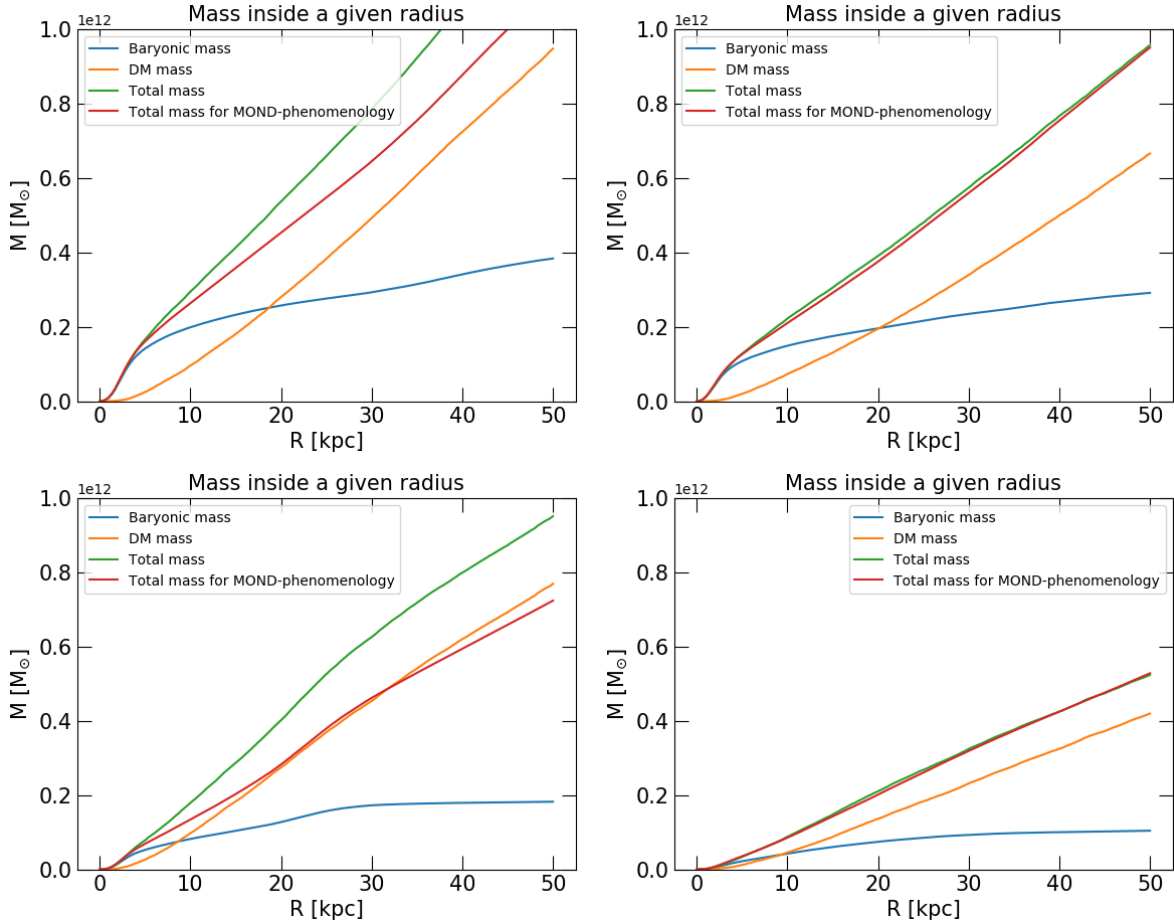


**Fig. 29:** Mass profiles of Magneticum galaxies. from top left to bottom right: 28,26,105,172.

As it was to be expected from the rotation curves in figure 9, the DM distributions of galaxy 36 and 172 almost exactly mimic the MOND law. Galaxy 28 and 105 show rather the opposite scenario, with there being far too much DM to reproduce MOND. It can be seen (more pictures in the appendix) that the magnitude of differences between the actual and the MOND-predicted halo vary substantially. MOND does over- and underpredict halos, and sometimes is extremely close to the real answer. In an observational setting, uncertainties - especially the MLR - can significantly affect the MOND prediction. For simulated galaxies, better agreement can often be reached by adjusting observational parameters such as the MLR appropriately [Dutton et al. (2019)], meaning that deviations from the MDAR could exist undetected in nature.

## 4.2 Baryonic mass profiles from MOND and halo shapes

When constructing a model of the DM in a galaxy, one has to start from observations of the dynamics of gas and stars and use these to constrain the model of the halo profile.

The general shape of that profile should of course be one that actually occurs in cosmological simulations, not just any shape is possible theoretically.

We can follow the opposite route: How do the baryonic and halo mass models of a galaxy need to be tweaked to get a MOND force law? Of course the baryonic density is somewhat constrained through observations.

Let us begin with the NFW halos in figures 5 and 6. Using (22) we can derive the baryonic mass and density the galaxy would need to emulate MOND with some interpolation function; I will use the simple interpolation function again.

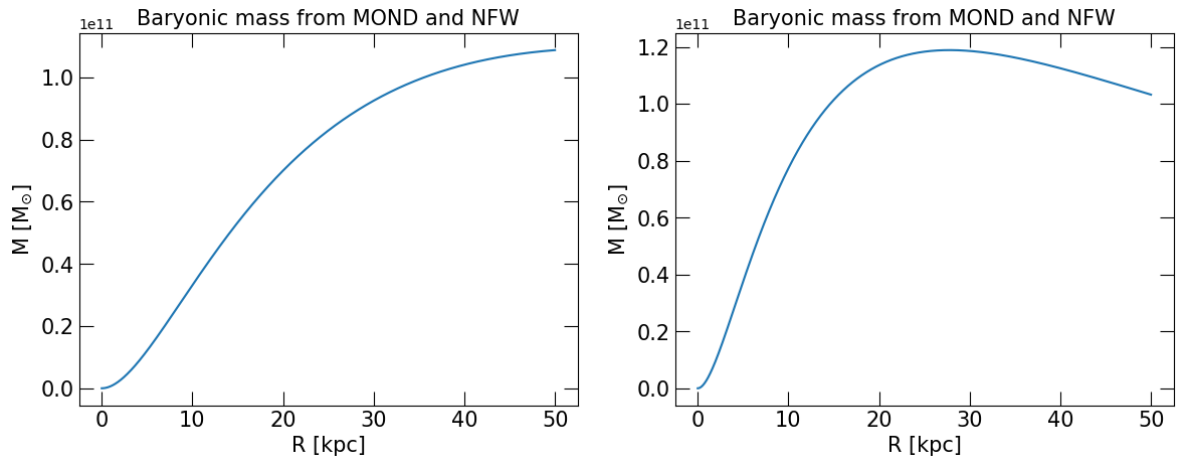


**Fig. 30:** Baryonic mass from NFW profile. Left:  $\rho_0 = 1 * 10^7 M_{\odot}/kpc^3, r_s = 20kpc$ . Right:  $\rho_0 = 1 * 10^8 M_{\odot}/kpc^3, r_s = 7kpc$ .

The second plot has the problem that for a declining curve to work in MOND, the enclosed mass would need to *decrease* at higher radii, which is clearly not possible. This showcases the incompatibility of declining rotation curves with MOND.

The same can be done for the Einasto profiles:

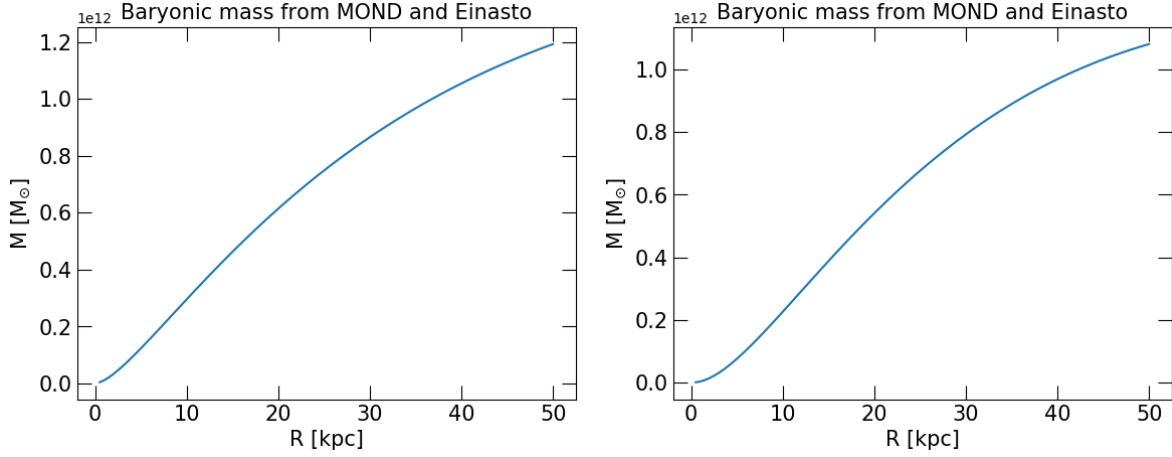


**Fig. 31:** Baryonic mass from Einasto profile.  $\rho_0 = 1 * 10^7 M_\odot / \text{kpc}^3$ ,  $r_s = 20 \text{kpc}$  for both. Left :  $\alpha=0.12$ . Right:  $\alpha=0.25$ .

Generally in regions of high acceleration, the baryonic mass forms the principal part of the total mass. When going out to lower accelerations, MOND of course predicts an increase of the mass-discrepancy. The baryonic mass calculated in this way is therefore much more concentrated than the DM halo itself, matching the  $\Lambda$ CDM prediction.

### 4.3 Acceleration laws in a Milky Way model

In constructing a somewhat more realistic model of a galaxy with stars, gas and DM, I followed a section of *Galactic Dynamics*, where a model of the Milky Way is laid out<sup>16</sup>. The idea here is to showcase how the MDAR varies with the baryonic and DM parameters.

This model includes all the basic parts of spiral galaxies:

- a) A central **bulge** of mostly older stars, with density given by

$$\rho_b(R, z) = \rho_{b0} \left( \frac{m}{a_b} \right)^{-\alpha_b} e^{-\frac{m^2}{r_b^2}}$$

with  $m = \sqrt{R^2 + \frac{z^2}{q_b^2}}$ .

- b) A **dark halo** in the form of a double power law:

$$\rho_h(R, z) = \rho_{h0} \left( \frac{m}{a_h} \right)^{-\alpha_h} \left( 1 + \frac{m}{a_h} \right)^{\alpha_h - \beta_h}$$

with  $m = \sqrt{R^2 + \frac{z^2}{q_h^2}}$ . Notice that we get an NFW for  $q_h = 1$ ,  $\alpha_h = 1$ ,  $\beta_h = 3$ .

<sup>16</sup>Galactic Dynamics p. 113

c) An exponential **stellar disk**, including a thick and thin disk component. Since the difference between the distribution of the two components lies in their in scale-heights perpendicular to the galactic plane and we are only interested in the rotation in the plane, I simplified to one component:

$$\rho_d(R, z) = \frac{\Sigma_d}{2z_0} e^{-\frac{R}{R_d} - \frac{|z|}{z_0}}$$

d) The **interstellar medium**, i.e. gas, with an optional central hole in the gas disk:

$$\rho_g = \frac{\Sigma_g}{2z_g} e^{-\frac{R}{R_g} - \frac{R_m}{R} - \frac{|z|}{z_0}}$$

There are many parameters in this model which determine the shapes and total masses of the individual components. For an explanation of the significance of these parameters, see the book and the associated paper [Dehnen and Binney (1998)].

I used models 1 and 2 from that very section of the book, which are models I and III here. Then I added two models of my own, denoted model II and IV. These only have one goal: To reproduce the MDAR predicted by MOND, with baryonic distributions the same as in I and III, respectively.

The parameters of the different models are:

	Model I	Model II	Model III	Model IV
$R_d$	2	2	3.2	3.2
$(\Sigma_d + \Sigma_g)[M_\odot kpc^{-2}]$	1905	1905	536	536
$\rho_{b0}[M_\odot kpc^{-3}]$	0.427	0.427	0.300	0.300
$\rho_{h0}[M_\odot kpc^{-3}]$	0.711	0.800	0.266	0.220
$\alpha_h$	-2.00	-0.90	1.63	0.70
$\beta_h$	2.96	2.03	2.17	2.10
$a_h[kpc]$	3.83	1.00	1.90	1.80

$\alpha_b = 1.8, q_b = 0.6, r_b = 1.9kpc, a_b = 1, q_h = 0.8, z_0 = 0.3kpc, z_g = 0.08kpc, R_m = 4kpc, R_g = 2R_d$  are the same for all models. I also kept the assumption that the gas contributes 25% of the baryonic surface density at the solar radius  $R_0 = 8kpc$ . The results were calculated using the approximation (9).

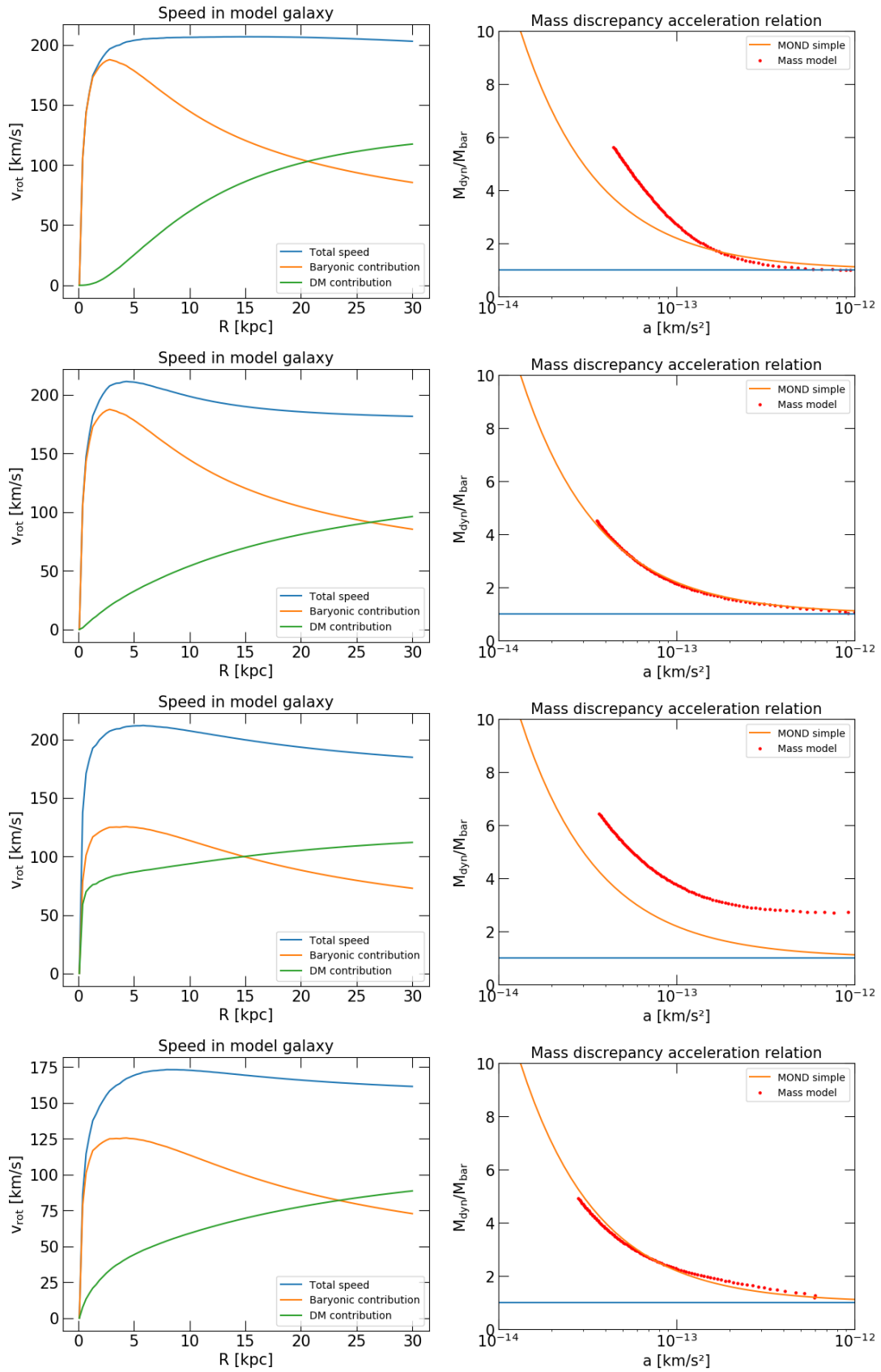


Fig. 32: From top to bottom: Model I-IV.

Notice how the total rotation curve of model II looks more like that of model III, while the decomposition into components more closely resembles model I. The models I and III are not based on dynamical data out to 30 kpc, therefore discrepancies between them in the outer regions are not surprising. I included these regions to broaden the range of accelerations.

The close match in the MDAR in models II and IV was achieved by simply playing around with the parameters of the halo in model I and III until they fit. Unsurprisingly, the outer regions, or the left side of the MDAR plot, are controlled by  $\beta_h$  and the inner regions by  $\alpha_h$ , while the turnover point depends on  $a_h$ . The MDAR is very sensitive to changes in  $\beta_h$  and  $\alpha_h$ .

Since model II lies entirely above the MOND MDAR, I needed to reduce the contribution of the halo for model IV at all radii. With unchanged baryonic mass profile, this of course meant changing the rotation curve to lower velocities. Model 1 did not require such substantial changes, mainly adjustments in the inner and outer slope, keeping the rotation curve similar.

There are probably a lot of ways to manipulate the halo shape in such a way that leads to this kind of agreement in the MDAR: While the mass distribution is uniquely determined by the MOND MDAR, there are four parameters to work with in the halo to get to that mass distribution.

What actually matters is whether the resulting halo shapes are realistic - this was not taken into account here and will not be looked at in this thesis.

#### 4.4 General results for mass distributions and the MDAR

It would be interesting to get an idea about how the matching of halo shape and baryonic mass distribution can be done in general, **preserving the shape of the rotation curve** of an observed galaxy.

Of course when the baryonic mass profile is exactly known, only one DM mass profile will do, because there is a one-to-one correspondence - but this is never the case in observations.

We start with the rotation curve because that is what can most reliably be measured. The total mass is given through the rotation curve, via (23). But the contribution of the baryonic component is not determined without an MLR, though the shape of the baryonic profile (for example the exponential scale radius of the disk) may be gained from luminosity observations. One usually has different MLRs for bulge, disk etc. - remember that this was assumed in this very thesis for the SPARC data.

Since the baryonic mass profile is then not fully specified, this gives legroom to ask the question: Knowing the rotation curve, what would the halo have to look like to give the MDAR of MOND?

Using the form of the MDAR for the simple interpolation function along with (23) and

assuming spherical symmetry, the mass distribution needed to exactly get the MDAR of MOND with the simple interpolation function for a given rotation curve is:

$$\begin{aligned} \frac{v^2(r)r}{G} &= M_{dyn}(r) = M_{bar}(r) + \frac{a_0 r^2}{G} \frac{M_{bar}(r)}{M_{dyn}(r)} \\ \Rightarrow M_{bar}(r) &= \frac{M_{dyn}^2(r)}{\frac{a_0 r^2}{G} + M_{dyn}(r)} = \frac{v^2(r)r}{G} \frac{1}{1 + \frac{a_0 r}{v^2(r)}} \end{aligned} \quad (34)$$

Since the total mass is baryons + halo, this gives:

$$M_{DM}(r) = \frac{v^2(r)r}{G} \frac{1}{1 + \frac{v^2(r)}{a_0 r}} = \frac{1}{G} \frac{r^2}{\frac{r}{v^2(r)} + \frac{1}{a_0}} \quad (35)$$

The mass distribution for a given (spherical!) double-power-law density of the halo can be calculated by evaluating the integral (dropping the subscript  $h$  that was used in the previous part)

$$M_{DM}(r) = 4\pi\rho_0 a^3 \int_0^{\frac{r}{a}} ds \frac{s^{2-\alpha}}{(1+s)^{\beta-\alpha}} \quad (36)$$

for the given values of  $\alpha, \beta, \rho_0, a$ .

A short demonstration of formula (35):

In the outer regions with low acceleration and  $v = const$ , the DM mass from (35) goes  $M(r) \sim r$  (since  $a_0 \gg \frac{v^2}{r}$ ), which leads to  $\rho(r) \sim r^{-2}$ . In the inner regions with higher acceleration, where  $v \sim r$ , we get  $M(r) \sim r^2$  (since  $a_0 \ll \frac{v^2}{r}$ ), leading to  $\rho(r) \sim r^{-1}$ . This gives a double-power-law halo with  $\alpha = 1, \beta = 2$ . In the inner regions, this is an NFW. But outside it cannot be, since the NFW has a declining curve at high radii, which MOND does not allow for.

Of course the accuracy of MOND here relies on the notion that rotation curves actually do not decline at large radii - which might not necessarily be the case, see for example [Namumba et al. (2018)].

One can even calculate the corresponding density directly using

$$\frac{\partial M_{DM}(r)}{\partial r} = 4\pi r^2 \rho(r). \quad (37)$$

Remembering that  $v = v(r)$ , we end up with this **MOND halo density profile** (DM density that emulates MOND for a given rotation curve):

$$\rho(r) = \frac{1}{4\pi G} \frac{\frac{1}{v^2} + \frac{2}{a_0 r} + \frac{2r}{v^3} \frac{\partial v}{\partial r}}{\left(\frac{r}{v^2} + \frac{1}{a_0}\right)^2} \quad (38)$$

The question may arise at this point what the above formulas are good for. The answer

is that if (35) and (36) generally match for a simulated galaxy with rotation curve  $v(r)$  and halo parameters  $\alpha, \beta, \rho_0, a$ , then MOND follows naturally from  $\Lambda$ CDM. The same holds for the densities. It would mean that MOND is able to predict halo shapes from cosmological simulations, where it is known for a fact that the shape of the rotation curve is a result of DM. This could signify MOND is at its heart an empirical relation that describes the relation between baryonic and dark mass distribution.

## 5 Summary

Galaxies from the Magneticum simulation were used to explore the difference in predictions between  $\Lambda$ CDM and MOND for disk galaxies.

Particular attention was given to three fundamental properties of spiral galaxies denoted the laws of galactic rotation.

Additionally, mass profiles of Magneticum galaxies and models for disk galaxies were studied and discussed in the context of acceleration relations predicted by MOND.

### 5.1 Laws of galactic rotation in Magneticum

The presence of the first law of galactic rotation in Magneticum is not surprising, as it is a fundamental part of the dark matter paradigm. Any remotely accurate  $\Lambda$ CDM simulation would necessarily have to capture flat asymptotic rotation curves.

But as we have seen, Magneticum also shows the different general shapes of rotation curves. An important difference I have shortly mentioned above is the decline of some DM curves at large radii, especially in galaxy 298 (see appendix). MOND cannot accommodate falling rotation curves - by virtue of the TFR (15) applicable in regions of low acceleration, MOND curves can only ever increase at larger radii.

The baryonic TFR or second law of galactic rotation does seem to be present to a limited degree. The important parameter is the exponent of the relation. While MOND predicts exactly 4, Magneticum gives approximately 3 for the whole mass range of the 'disks' with b-value greater -4.375. When a cutoff is made at  $10^{11}M_{\odot}$ , the exponent shrinks down to  $\frac{100}{29} \approx 3.45$ , which still is not compatible with MOND.

The authors of [Lelli et al. (2019)] come to the conclusion that the slope is  $3.85 \pm 0.09$  in the SPARC sample, although may be in the range 3.5 - 4 due to the systematic uncertainties. [Ponomareva et al. (2018)] on the other hand find a slope of  $2.99 \pm 0.22$  based on a different sample and stress the importance of the choice of MLR.

Detailed analysis should be done on the list of galaxies, making sure that really only disk galaxies are used here.

That leaves the acceleration relations stated as the third law. I explained before that this is the one that has the most power to show that MOND is not just empirical, but a fundamental property of the universe. But the presence of the specific form of the MDAR

and RAR predicted by MOND in Magneticum means that it need not be. Instead, it seems DM emulates MOND in some way. The presence of these relations not just in the collection of the data set (the 152 galaxies with  $b$ -value greater than  $-4.375$ ), but in some individual galaxies hints at the fact that it is actually the interaction of DM and baryons that is fundamental.

It seems as though the RAR from Magneticum might lie under the MOND prediction when approaching accelerations of  $\sim 10^{-14} km/s^2$ . This would echo a trend from [Dutton et al. (2019)]. But this part of the MDAR/RAR is very sparse in the Magneticum data, due to there being almost exclusively high mass galaxies to analyze.

Also, high mass galaxies seem to deviate most clearly from the MDAR/RAR, predicting higher dynamical to baryonic mass ratios than MOND.

The scatter in the MDAR from Magneticum is actually somewhat lower than in the SPARC data set. Of course assuming the same intrinsic scatter, this is to be expected - no observational errors can contaminate the Magneticum data.

## 5.2 Mass distributions of galaxies in the context of the MDAR

By calculating the total mass profile a galaxy would need to reproduce the MOND MDAR from the baryonic mass, one has another way of visualizing how close the agreement between MOND and  $\Lambda$ CDM is in some galaxies. As expected, there is a match between galaxies where MOND and the DM profile predict similar rotation curves and ones where the total mass profile is close to the one calculated in this way.

This connection can also be approached from the other direction by 'deriving' a baryonic mass profile from a given halo shape.

A comparison could be made between these and realistic baryonic mass profiles in the future.

A simple model of the Milky Way showcases that when the baryonic mass is known, whether a halo shape can be found that both preserves the rotation curve (within a range of uncertainty) *and* shows the MOND MDAR depends on the shape of the rotation curve. When the mass discrepancy is higher (or lower) than predicted by MOND at all radii, there is no possibility of finding a halo that does both.

In observations, the baryonic mass is obviously never completely known. Therefore it is not unreasonable to calculate which halo mass and density profiles could produce an observed rotation curve *and* the MOND MDAR. The results are the formulas (35) and (38) above.

A widespread agreement between halos given by these formulas and the 'actual' halos of simulated galaxies with a given rotation curve would mean MOND phenomenology is expected to arise in  $\Lambda$ CDM.

We know from the MDAR in Magneticum that there has to be some level of match. But a general discussion of halo shapes in cosmological simulations or even in Magneticum is clearly beyond the scope of this thesis.

## 6 Conclusions and outlook

### 6.1 Implications

What is the significance of the presence of MOND phenomenology in  $\Lambda$ CDM simulations? From the standpoint of MOND, this result can be surprising: Why should a characteristic dependence of the mass/acceleration discrepancy - which is, as [McGaugh (2014)] puts it, "uniquely predicted by MOND" - also exist in simulations with dark matter, but no acceleration-dependent modification of the force-law? MOND is certainly not directly written into  $\Lambda$ CDM simulations in any way.

But viewed from the perspective of the standard model, this result is not surprising at all (although it may certainly be reassuring). If the standard model is correct and we actually live in a universe dominated by dark matter, then MOND is simply a fit to observations which are a result of how dark matter and baryonic matter interact during galaxy formation and evolution.

If it is found that the occurrence of MOND is a general trend in  $\Lambda$ CDM simulations, then MOND could be used to predict halo shapes from rotation curves. This would actually echo a claim made by proponents of MOND [McGaugh et al. (2016)], but would take on a new significance in this context.

It seems we have arrived at scenario a) from the introduction - predictions by MOND also hold true for galaxies with dark matter from cosmological simulations. Therefore it appears that both MOND and  $\Lambda$ CDM predict a similar form of the RAR/MDAR. These relations are therefore not exclusive evidence for one or the other, rendering a distinction on this basis impossible.

Nonetheless, I will repeat my statement from the introduction that this result is very consistent with the notion that MOND is purely an empirical relation found from a  $\Lambda$ CDM universe. It certainly invalidates the claim of [McGaugh (2015)] that the  $\Lambda$ CDM model "clearly fails" because it does not show the MDAR/RAR observed in nature.

In McGaugh (2014), it is argued that the laws of galactic rotation may be seen as being analogous to Kepler's laws of planetary motion, which were solely empirical in nature, but subsequently explained by Newton's law of universal gravitation along with the rest of Newtonian dynamics. Of course in this case, the fundamental law would be the MOND force-law.

But the presence of MOND phenomenology in  $\Lambda$ CDM-simulations could hint at a different interpretation: Namely, that MOND is similar to Kepler's laws, and the standard model of cosmology similar to Newton's law of gravitation in this analogy, because the observed acceleration scaling seems to be a consequence of the galaxy formation in  $\Lambda$ CDM. If this interpretation is correct, then insisting that MOND is the fundamental law is akin to saying that although Newton's law can explain the three laws of planetary motion and makes correct predictions in other areas, planets just fundamentally orbit the sun in ellipses - no Newtonian gravity needed.

## 6.2 Other tests for MOND

While it seems that the predictions of  $\Lambda$ CDM and MOND might be similar on the scale of galaxies, there are ways to distinguish quite conclusively between a modified force law and dark matter. The rotation speeds of wide binaries have been suggested and used as a test for a while [Hernandez et al. (2012)], but recent data releases from GAIA have allowed researchers to look at these binary systems much closer than ever before [Pittordis and Sutherland (2019)].

The idea is that in stark contrast to galactic dynamics, DM is not thought to play much of a role in the internal dynamics of a binary star system, as the dark matter is about homogeneously distributed over such a small part of the galaxy. Therefore, detecting a deviation from Newtonian dynamics here would tip the scale quite clearly for MOND.

Alas, [Pittordis and Sutherland (2019)] come to the conclusion that still more data is needed.

In principle, any time there is low acceleration (with the caveat there be no influence from DM) there is a test for MOND. So even future tests on earth might be possible [Ignatiev (2015)].

Seeing as the distinction between DM and MOND has proven to be difficult in galaxies, these other tests seem promising as an alternative.

Of course there is always the possibility of the detection of a suitable DM particle. This would at the very least invalidate one of the greatest critiques of  $\Lambda$ CDM. But this detection would also not necessarily disprove MOND - MOND can include some smaller amount of dark mass.

## 6.3 Building upon this thesis

There are clearly many things left to do here. One of the most fundamental questions left open is whether the merger history of galaxies which emulate MOND well is generally different from those who do not.

This leads to the issue of MOND at different values of redshift: If the formation history is central, then younger galaxies might show different acceleration laws.

Generally, the extraction of data from *Magneticum* should be done in a way that more closely resembles observations. First off, the velocities could be measured as the line-of-sight velocity from a randomly stationed observer, mimicking uncertainties in circular speed measurements. See the appendix for a basic attempt to perform this process. Next, the baryonic mass model could also be constructed with the limited data an observer has at his or her hands. This especially concerns the MLR, as MOND predictions

depend critically on it.

The possibility of predicting halo shapes with the use of MOND should also be investigated, as this may lead to a greater understanding of the connection between rotation curves and DM halos.

## 7 Appendix

### 7.1 Simulating observation

Over the course of this thesis, the rotation curves from the simulation were directly derived from the output which includes the position and velocity vector for every particle. In actual observations of distant galaxies, or even the Milky Way, this wealth of information is not available. Instead, the measured quantity is the **Line-of-sight velocity (LOSV)**, which is the projection of the velocity vector onto the line of sight. Measuring Doppler-shifts, one can obtain a 2D-map of the LOSV. The actual rotation curve is then usually obtained from fitting a **Tilted Ring Model (TRM)** to the velocity map, as I explained in the body of the thesis.

The LOSV-map is obtained from the projection of the velocity vectors of the gas particles here.

The TRM-fit was also used on much the SPARC-data set [Lelli et al. (2016)]. Therefore, to improve the ability to compare this data to the results of *Magneticum*, a similar, but simplified procedure was tried out to obtain rotation curves from the *Magneticum* galaxies. In contrast to the usual TRM, only a single value for the inclination and the position angle was used for the whole galaxy. Because of these changes, this method would more fittingly be described as an inclined disk model, where the disk is still divided into rings with different values of the circular velocity.

Unfortunately, this method did not work sufficiently well to allow me to use the TRM instead of the procedure used in the body of the thesis. Sometimes the fit just fails completely and returns the starting values for the fit. And the velocities are far too low in general.

Below are some examples. The discrepancy in velocities between velocity map and model is clearly visible. To get better speed-models, an improved fitting-algorithm is probably needed. It should be noted, however, that one will necessarily encounter problems fitting a model to a nearly face-on galaxy and those will sometimes occur in this method, as they do in nature.

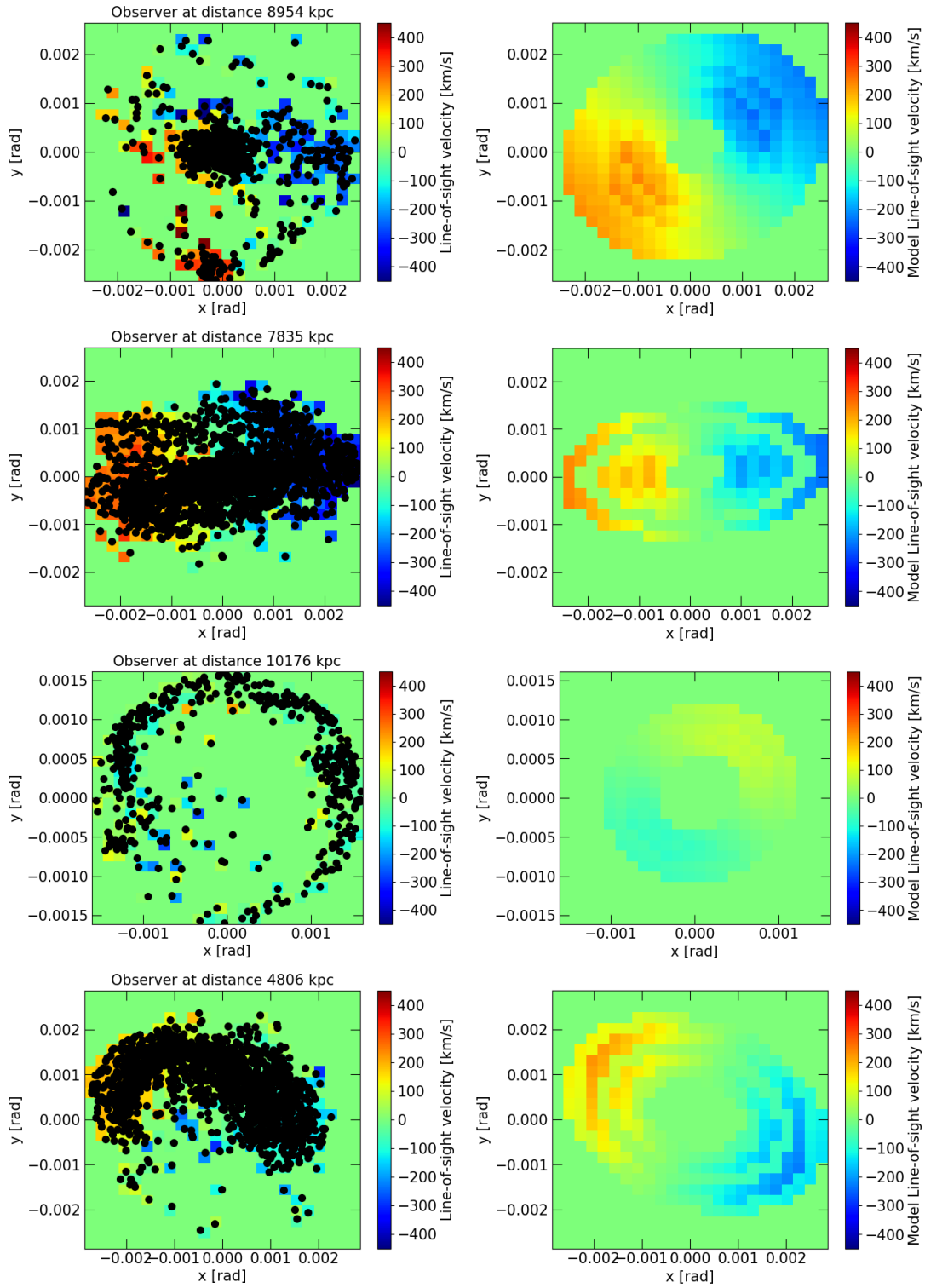


**Fig. 33:** Velocity maps and models for different galaxies. From top to bottom: 28,36,105,172.

## 7.2 Additional plots

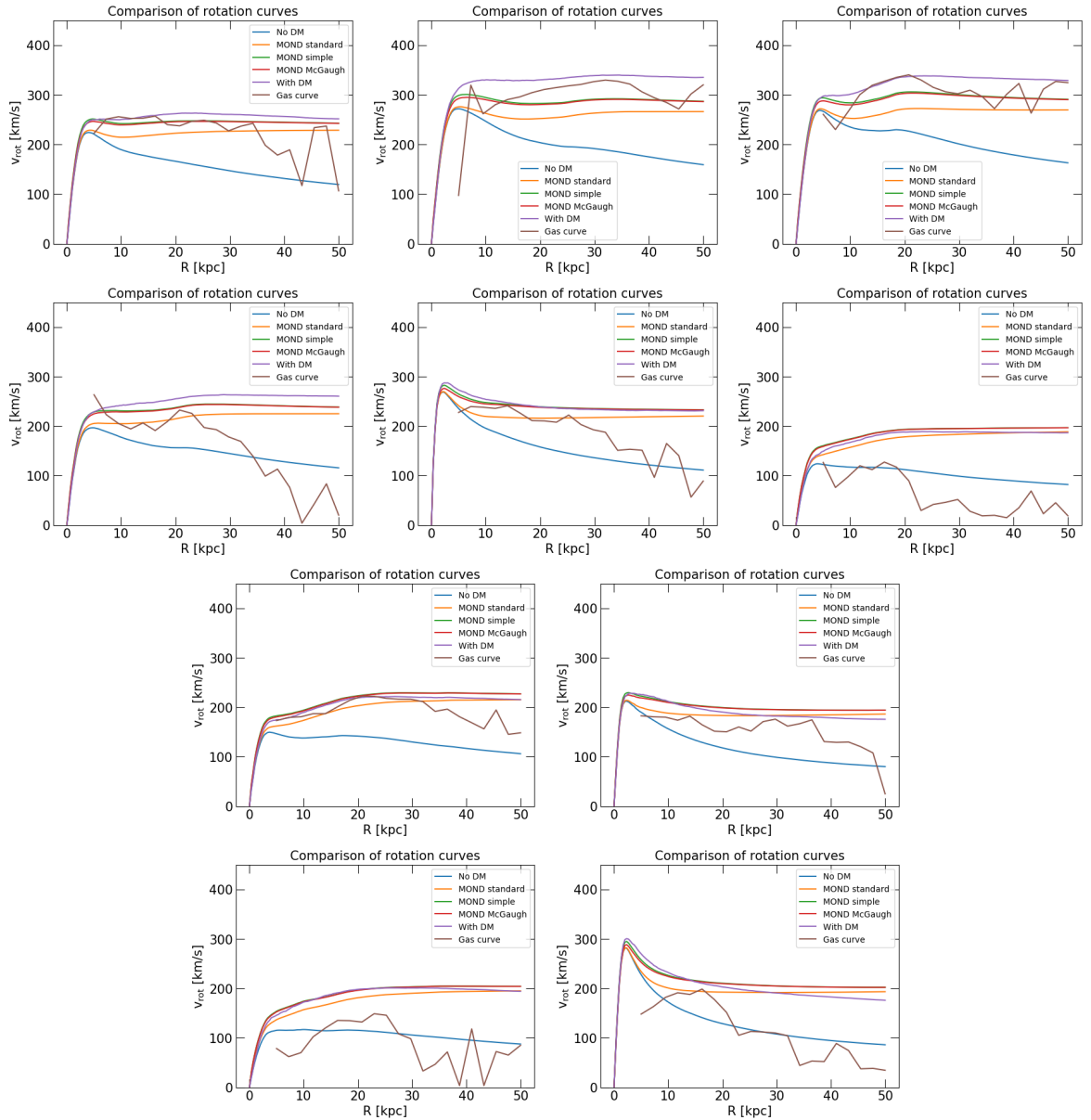
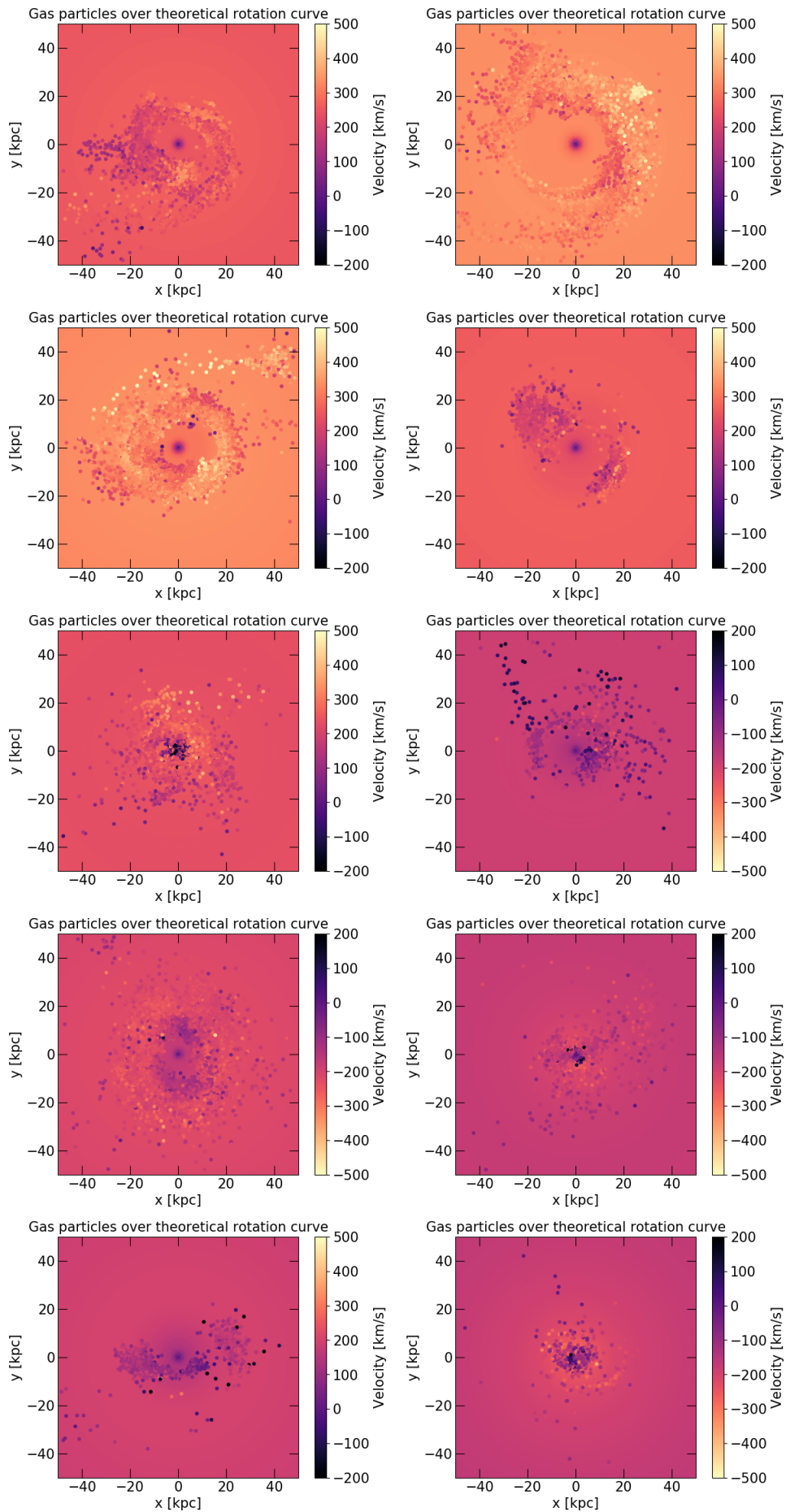
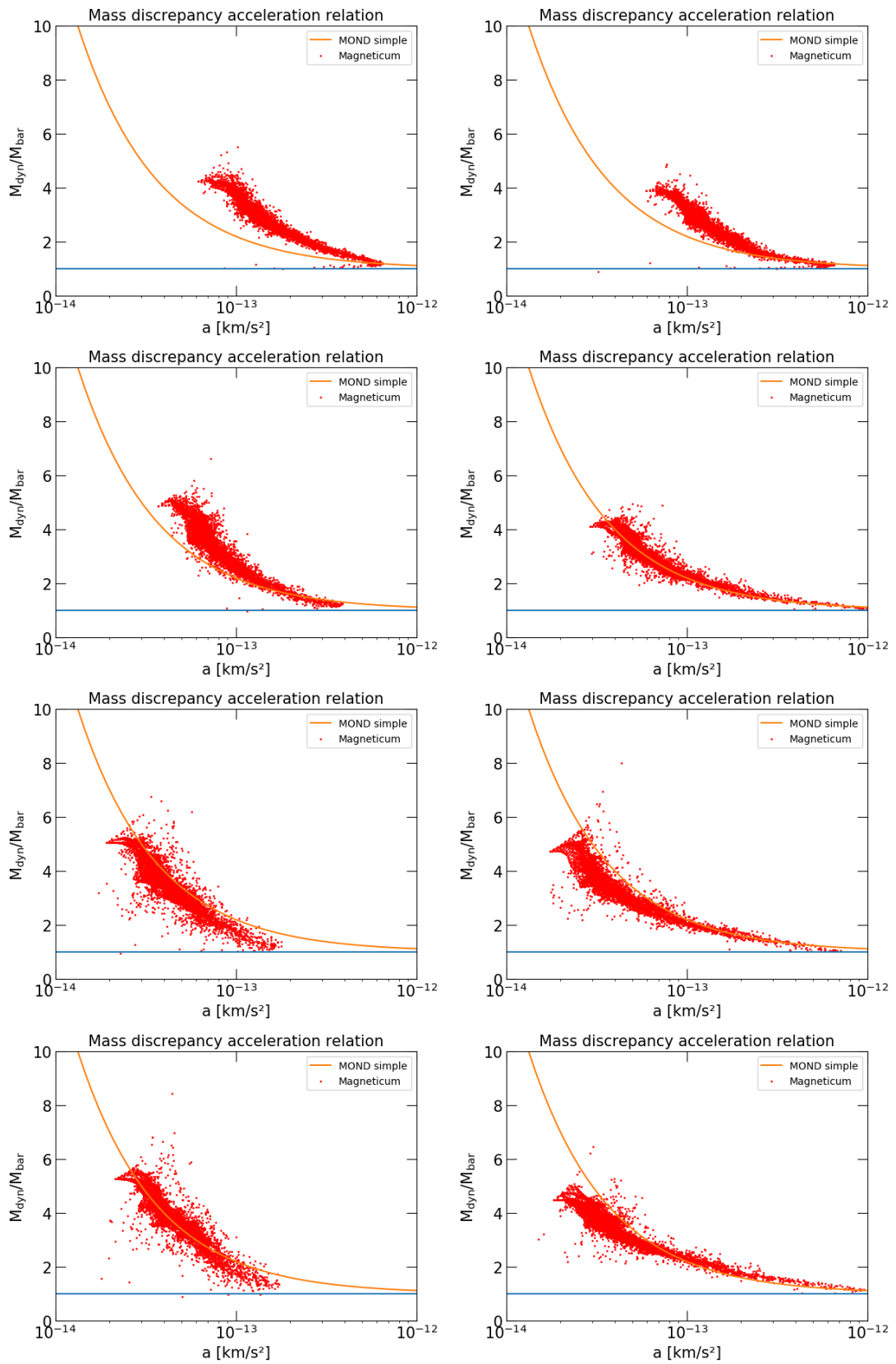


Fig. 34: Top left to bottom right: 20,40,41,84,115,124,202,264,269,298.



**Fig. 35:** Top left to bottom right: 20,40,41,84,115,124,202,264,269,298



**Fig. 36:** Top left to bottom right: 40,41,84,115,124,264,269,298

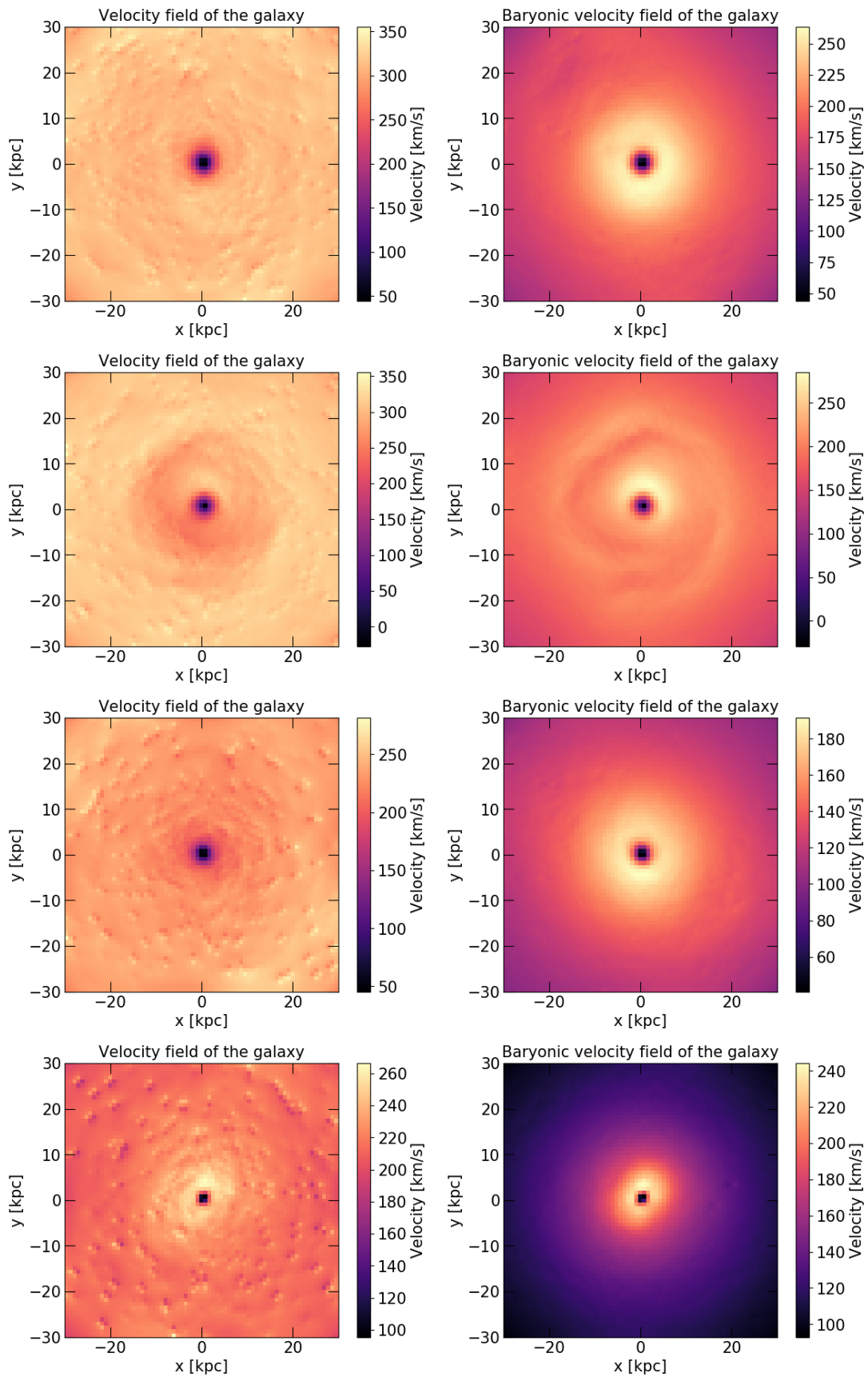
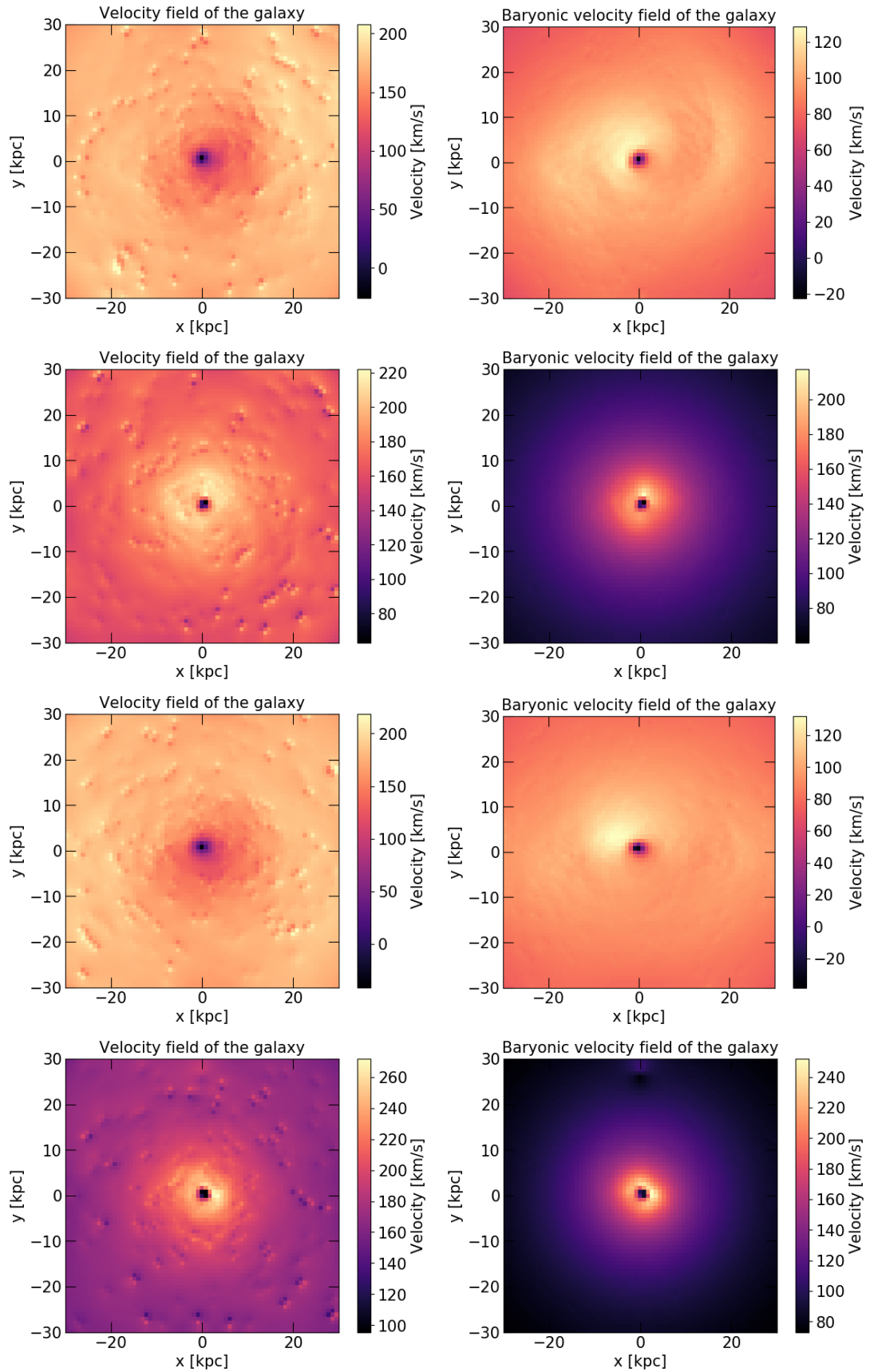


Fig. 37: Top to bottom: 40,41,84,115



**Fig. 38:** Top to bottom: 124,264,269,298

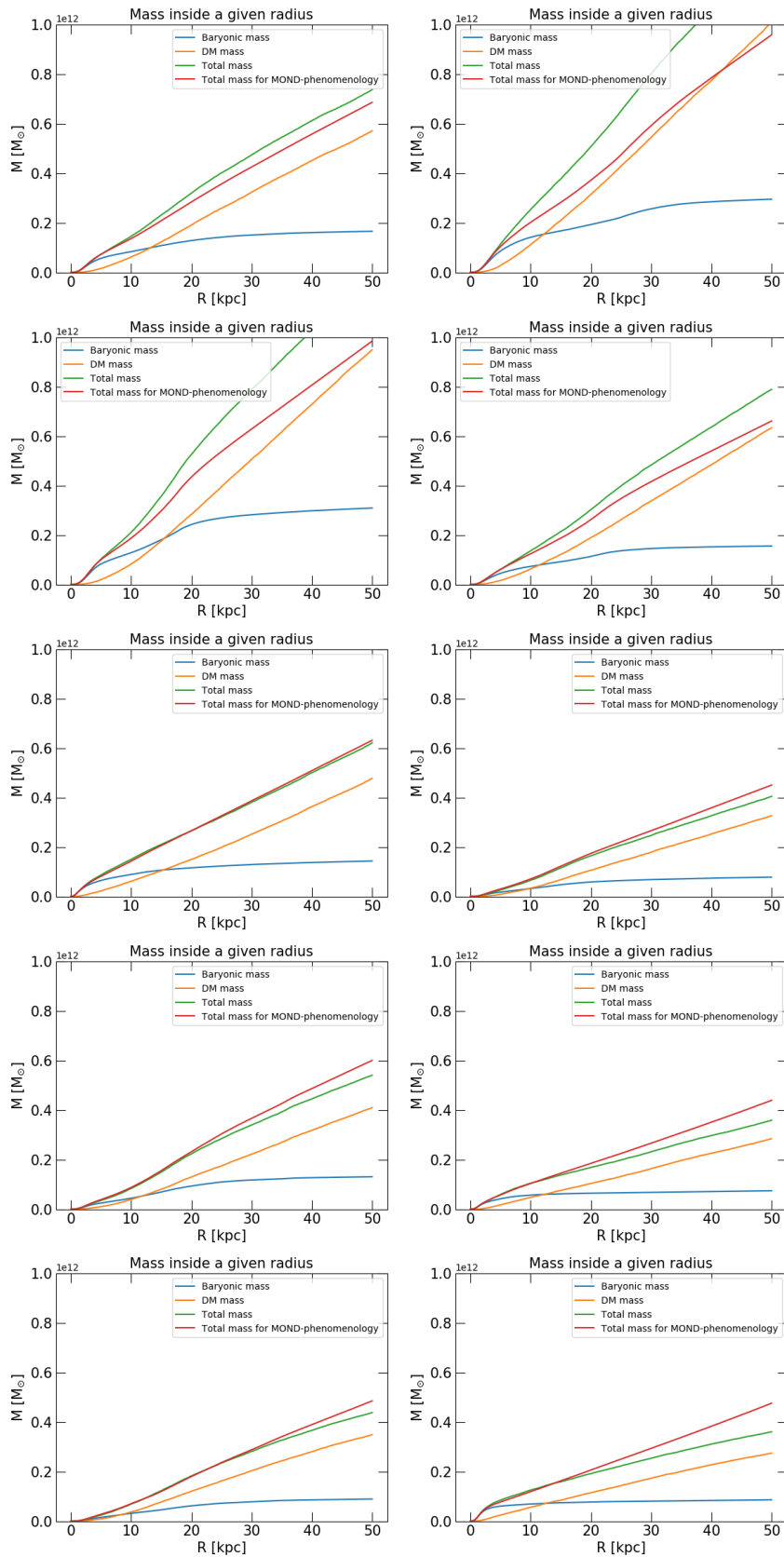


Fig. 39: Top left to bottom right: 20,40,41,84,115,124,202,264,269,298

# Bibliography

- Alpher, R. A. and Herman, R. (1948). Evolution of the Universe. *Nature*, 162(4124):774–775.
- Bekenstein, J. D. (2004). Relativistic gravitation theory for the modified Newtonian dynamics paradigm. *Physical Review D*, 70(8):083509.
- Bland-Hawthorn, J. and Gerhard, O. (2016). The Galaxy in Context: Structural, Kinematic, and Integrated Properties. *Annual review of astronomy and astrophysics*, 54:529–596.
- Dehnen, W. and Binney, J. (1998). Mass models of the Milky Way. *Monthly Notices of the Royal Astronomical Society*, 294(3):429–438.
- Dolag, K., Vazza, F., Brunetti, G., and Tormen, G. (2005). Turbulent gas motions in galaxy cluster simulations: the role of smoothed particle hydrodynamics viscosity. *Monthly Notices of the Royal Astronomical Society*, 364(3):753–772.
- Dutton, A. A., Macciò, A. V., Obreja, A., and Buck, T. (2019). NIHAO - XVIII. Origin of the MOND phenomenology of galactic rotation curves in a  $\Lambda$ CDM universe. *Monthly Notices of the Royal Astronomical Society*, 485(2):1886–1899.
- Einstein, A. (1905). Zur Elektrodynamik bewegter Körper. *Annalen der Physik*, 322:891–921.
- Fixsen, D. J. (2009). The Temperature of the Cosmic Microwave Background. *The Astrophysical Journal*, 707(2):916–920.
- Friedmann, A. (1922). Über die Krümmung des Raumes. *Zeitschrift für Physik*, 10:377–386.
- Gamow, G. (1948). The Evolution of the Universe. *Nature*, 162(4122):680–682.
- Hernandez, X., Jiménez, M. A., and Allen, C. (2012). Wide binaries as a critical test of classical gravity. *European Physical Journal C*, 72:1884.
- Hubble, E. (1929). A Relation between Distance and Radial Velocity among Extra-Galactic Nebulae. *Proceedings of the National Academy of Science*, 15(3):168–173.
- Ignatiev, A. Y. (2015). Testing MOND on Earth. *Canadian Journal of Physics*, 93(2):166–168.

- Kapteyn, J. C. (1922). First Attempt at a Theory of the Arrangement and Motion of the Sidereal System. *The Astrophysical Journal*, 55:302.
- Kiselev, V. V. and Timofeev, S. A. (2012). Cosmological extrapolation of modified Newtonian dynamics. *Classical and Quantum Gravity*, 29(6):065015.
- Komatsu, E., Smith, K. M., Dunkley, J., Bennett, C. L., Gold, B., Hinshaw, G., Jarosik, N., Larson, D., Nolte, M. R., and Page, L. (2011). Seven-year Wilkinson Microwave Anisotropy Probe (WMAP) Observations: Cosmological Interpretation. *The Astrophysical Journal Supplement*, 192(2):18.
- Lelli, F., McGaugh, S. S., and Schombert, J. M. (2016). SPARC: Mass Models for 175 Disk Galaxies with Spitzer Photometry and Accurate Rotation Curves. *Astronomical Journal*, 152(6):157.
- Lelli, F., McGaugh, S. S., Schombert, J. M., Desmond, H., and Katz, H. (2019). The baryonic Tully-Fisher relation for different velocity definitions and implications for galaxy angular momentum. *Monthly Notices of the Royal Astronomical Society*, 484(3):3267–3278.
- Lelli, F., McGaugh, S. S., Schombert, J. M., and Pawlowski, M. S. (2017). One Law to Rule Them All: The Radial Acceleration Relation of Galaxies. *The Astrophysical Journal*, 836(2):152.
- Lemaître, G. (1927). Un Univers homogène de masse constante et de rayon croissant rendant compte de la vitesse radiale des nébuleuses extra-galactiques. *Annales de la Société Scientifique de Bruxelles*, 47:49–59.
- McGaugh, S. (2014). The Third Law of Galactic Rotation. *Galaxies*, 2(4):601–622.
- McGaugh, S. S. (2005). Balance of Dark and Luminous Mass in Rotating Galaxies. *Physical Review Letters*, 95(17):171302.
- McGaugh, S. S. (2015). A tale of two paradigms: the mutual incommensurability of  $\Lambda$ CDM and MOND. *Canadian Journal of Physics*, 93(2):250–259.
- McGaugh, S. S., Lelli, F., and Schombert, J. M. (2016). Radial Acceleration Relation in Rotationally Supported Galaxies. *Physical Review Letters*, 117(20):201101.
- McGaugh, S. S. and Schombert, J. M. (2015). Weighing Galaxy Disks With the Baryonic Tully-Fisher Relation. *The Astrophysical Journal*, 802(1):18.
- Merritt, D. (1987). The Distribution of Dark Matter in the Coma Cluster. *The Astrophysical Journal*, 313:121.
- Milgrom, M. (1983a). A modification of the Newtonian dynamics - Implications for galaxies. *The Astrophysical Journal*, 270:371–389.

- Milgrom, M. (1983b). A modification of the newtonian dynamics : implications for galaxy systems. *The Astrophysical Journal*, 270:384–389.
- Milgrom, M. (1983c). A modification of the Newtonian dynamics as a possible alternative to the hidden mass hypothesis. *The Astrophysical Journal*, 270:365–370.
- Namumba, B., Carignan, C., and Passmoor, S. (2018). H I observations of Sextans A and B with the SKA pathfinder KAT-7. *Monthly Notices of the Royal Astronomical Society*, 478(1):487–500.
- Navarro, J. F., Benítez-Llambay, A., Fattahi, A., Frenk, C. S., Ludlow, A. D., Oman, K. A., Schaller, M., and Theuns, T. (2017). The origin of the mass discrepancy-acceleration relation in  $\Lambda$ CDM. *Monthly Notices of the Royal Astronomical Society*, 471(2):1841–1848.
- Navarro, J. F., Frenk, C. S., and White, S. D. M. (1996). The Structure of Cold Dark Matter Halos. *The Astrophysical Journal*, 462:563.
- Penzias, A. A. and Wilson, R. W. (1965). A Measurement of Excess Antenna Temperature at 4080 Mc/s. *The Astrophysical Journal*, 142:419–421.
- Pittordis, C. and Sutherland, W. (2019). Testing Modified Gravity with Wide Binaries in GAIA DR2. *arXiv e-prints*, page arXiv:1905.09619.
- Planck Collaboration, Akrami, Y., Arroja, F., Ashdown, M., Aumont, J., Baccigalupi, C., Ballardini, M., Banday, A. J., Barreiro, R. B., and Bartolo, N. (2018). Planck 2018 results. I. Overview and the cosmological legacy of Planck. *arXiv e-prints*, page arXiv:1807.06205.
- Ponomareva, A. A., Verheijen, M. A. W., Papastergis, E., Bosma, A., and Peletier, R. F. (2018). From light to baryonic mass: the effect of the stellar mass-to-light ratio on the Baryonic Tully-Fisher relation. *Monthly Notices of the Royal Astronomical Society*, 474(4):4366–4384.
- Ponomareva, A. A., Verheijen, M. A. W., Peletier, R. F., and Bosma, A. (2017). The multiwavelength Tully-Fisher relation with spatially resolved H I kinematics. *Monthly Notices of the Royal Astronomical Society*, 469(2):2387–2400.
- Riess, A. G., Filippenko, A. V., Challis, P., Clocchiatti, A., Diercks, A., Garnavich, P. M., Gilliland, R. L., Hogan, C. J., Jha, S., and Kirshner, R. P. (1998). Observational Evidence from Supernovae for an Accelerating Universe and a Cosmological Constant. *Astronomical Journal*, 116(3):1009–1038.
- Sanders, R. H. and McGaugh, S. S. (2002). Modified Newtonian Dynamics as an Alternative to Dark Matter. *Annual review of astronomy and astrophysics*, 40:263–317.
- Sofue, Y. and Rubin, V. (2001). Rotation Curves of Spiral Galaxies. *Annual review of astronomy and astrophysics*, 39:137–174.

- Springel, V. (2005). The cosmological simulation code GADGET-2. *Monthly Notices of the Royal Astronomical Society*, 364(4):1105–1134.
- Springel, V., Di Matteo, T., and Hernquist, L. (2005). Modelling feedback from stars and black holes in galaxy mergers. *Monthly Notices of the Royal Astronomical Society*, 361(3):776–794.
- Springel, V. and Hernquist, L. (2003). Cosmological smoothed particle hydrodynamics simulations: a hybrid multiphase model for star formation. *Monthly Notices of the Royal Astronomical Society*, 339(2):289–311.
- Teklu, A. F., Remus, R.-S., Dolag, K., Beck, A. M., Burkert, A., Schmidt, A. S., Schulze, F., and Steinborn, L. K. (2015). Connecting Angular Momentum and Galactic Dynamics: The Complex Interplay between Spin, Mass, and Morphology. *The Astrophysical Journal*, 812(1):29.
- Tully, R. B. and Fisher, J. R. (1977). Reprint of 1977A&A...54..661T. A new method of determining distance to galaxies. *Astronomy & Astrophysics*, 500:105–117.
- Weinberg, S. (1989). The cosmological constant problem. *Reviews of Modern Physics*, 61(1):1–23.
- Wiersma, R. P. C., Schaye, J., Theuns, T., Dalla Vecchia, C., and Tornatore, L. (2009). Chemical enrichment in cosmological, smoothed particle hydrodynamics simulations. *Monthly Notices of the Royal Astronomical Society*, 399(2):574–600.
- Zwicky, F. (1933). Die Rotverschiebung von extragalaktischen Nebeln. *Helvetica Physica Acta*, 6:110–127.

**Books:**

- Binney, J. , Tremaine S. (2008). *Galactic Dynamics*. Princeton University Press, second edition.
- Binney, J. , Merrifield, M. (1998). *Galactic Astronomy*. Princeton University Press.
- Misner, C.W. , Thorne, K.S. , Wheeler, J.A. (2017). *Gravitation*. Princeton University Press, 2017 edition.
- Mo, H. , van den Bosch, F. , White, S. (2010). *Galaxy Formation and Evolution*. Cambridge University Press.
- Schneider, P. (2008). *Einführung in die Extragalaktische Astronomie und Kosmologie*. Springer.
- Unsöld, A. , Baschek, B. (2002). *Der neue Kosmos*. Springer Spektrum, seventh edition.

## Danksagung

Ich möchte mich bei allen bedanken, die mir bei der Erstellung dieser Bachelorarbeit geholfen haben.

Das betrifft zuerst einmal meine im Grunde drei Betreuer Adelheid, Rhea und Klaus, die mich durch ihr positives und motivierendes Feedback sehr unterstützt haben. Klaus möchte ich insbesondere dafür danken, dass er gleich durchschaut hat, dass mich dieses Thema interessieren würde.

Ich meine aber auch die gesamte CAST-Gruppe an der USM, die mich sofort freundlich aufgenommen und nie genervt auf meine vielen Fragen reagiert hat. Das geht besonders an Ludwig und Pascal, die mir immer bei meinen zahlreichen technischen Problemen weiterhelfen konnten.

Danke, dass ihr alle mir die Zeit so angenehm gemacht habt!

Nun kommen wir zu den Menschen hinter den Kulissen, die aber bekanntlich die entscheidenden sind:

Einen Riesendank an meine Eltern, die wie immer voll hinter mir und mir in Phasen von Schreibblockaden wie -flüssen zur Seite standen.

Und zuallerletzt, aber natürlich am wichtigsten: Meine Freundin Simone, die sich stets meine ewigen Erklärungen mit viel Verständnis und Liebe anhört und mir ihren cleveren Rat zurückgibt.

